



Department of Meteorology

**The role of moisture as a control on tropical
convection**

Cheong Wee Kiong

August 2009

A dissertation submitted in partial fulfillment of the requirement for the
degree of MSc Atmosphere, Ocean and Climate

Abstract

Several recent studies through observations demonstrated that there is a strong positive relationship between precipitation and column water vapour (CWV) over the tropical ocean. This report will investigate the robustness of this precipitation-CWV relationship from observation over tropical land and from model simulated data.

Twelve years of radiosonde and rain gauge data from Singapore are used to analyze the relationship between precipitation and relative column water vapour (RCWV). A steady increasing trend in precipitation with RCWV is indicated through all seasons. Moisture in the lower free troposphere is the key component in determining this precipitation-RCWV relationship. The 'strength' of the precipitation-RCWV relationship is likely to be affected by large scale moisture and precipitation advection; but not by the diurnal cycle in RCWV or the mean atmospheric temperature. A precipitation lag-lead analysis suggests positive moisture anomalies several hours before and after precipitation. These results indicate that moisture variation is playing a very important role in the variation in convection activities over tropical land.

Both 40km and 12km resolution runs from the UK met office Unified Model employed in this study simulate the steady increasing trend in precipitation-CWV relationship over both the tropical ocean and land reasonably well. Departure from the steady increasing trend over high elevated region highlights the temperature dependence on the precipitation-CWV relationship. A moisture budget analysis indicates that on an hourly timescale, diurnal variation in evaporation, moisture advection and precipitation all contribute to a large portion in moisture variation over the land; evaporation plays a minor role in the CWV variation over the ocean. On a daily timescale, the moisture variation is dominated by moisture advection and precipitation over both the ocean and land.

Although there is some variation in the contributing factors to changes in moisture content, the steady increasing trend in the precipitation-RCWV/CWV relationship holds over both the tropical oceans and land.

Acknowledgments

Heartfelt thanks to my supervisors Dr Robert S. Plant and Dr Christopher E. Holloway for their guidance in completing this project. I would also like to thank the National Environment Agency of Singapore for their scholarship which has allowed me to study this MSc course.

Contents

1	Tropical convection	1
1.1	Introduction	1
1.1.1	Role of tropical convection in global atmosphere	1
1.1.2	Importance of organized features	1
1.1.3	Representation of convection in numerical weather prediction	2
1.2	Factors controlling tropical convection.....	4
1.3	Role of moisture in controlling tropical convection.....	5
1.3.1	Relationships between tropospheric moisture (Column Water vapour) and Tropical Precipitation	5
1.3.2	Representation of tropospheric moisture in convective parameterization.....	7
	Project aims	8
2	Data description and categorization	10
2.1	Climatology of Singapore	12
2.2	Distribution of data set	14
3	Results I: Relationships between Relative column Water vapour and Tropical Precipitation (Sonde Observations)	16
3.1	Effect of precipitation on moisture structure	16

3.2	Rainfall Intensity conditioned on column water vapour and Relative column water vapour.....	17
3.2.1	Daily mean rainfall conditioned on Relative column Water Vapour (ENSO and Monsoons categorization)	18
3.3	Impact of temperature on moisture structure	22
3.4	Daily mean rainfall range per bin.....	27
3.5	Advection of moisture	30
3.6	Precipitation lag-lead analysis.....	35
4	Results II: Relationships between column Water vapour and Tropical Precipitation (Model simulations)	40
4.1	Introduction	40
4.1.1	Model descriptions	41
4.1.2	Weather highlights over the thirty day period	42
4.2	Relationship between precipitation and atmospheric moisture contents.....	42
4.2.1	Precipitation and column water vapour relationship (Domain mean)	43
4.2.2	Precipitation and column water vapour relationship (Grid points).....	45
4.3	Moisture budget	49
4.3.1	Impact of model resolution (hourly precipitation, evaporation rates and column water content).....	49
4.3.2	Impact of model resolution (Moisture budget: hourly domain mean).....	51
4.3.3	Contributing factors to moisture content (Hourly domain mean: Land/Ocean)	55

4.3.4	Moisture budget (Daily domain mean)	58
5	Conclusions and Summary	63
5.1	Summary of results.....	63
5.1.1	Results from observation	63
5.1.2	Results from model simulation	64
5.1.3	Conclusion	65
5.2	Project Limitations	66
5.3	Future works	66
	References and Appendices	68

Chapter 1 Tropical Convection

1.1 Introduction

1.1.1 Role of tropical convection in global atmosphere

Over two-thirds of the global precipitation falls in the tropics, and weather in the tropics is dominated by the effects of thermally driven cumulus convection. Deep convective systems (thermally driven turbulent mixing, where vertical motions take parcels from lower atmosphere above 500 hPa), associated with plentiful precipitation, are prominent features of the tropical atmosphere that have important roles at a spectrum of space and time scales from local diurnal cycles to the planetary-scale circulations. In addition to its dynamical importance for the tropical circulation, deep convection is the primary source of high clouds and upper-tropospheric water vapour, which strongly impact the radiation budget of the planet. Moist boundary layer air is transported by deep convection to the dry mid- and upper troposphere, where even slight humidity increases can strongly reduce the radiation emitted to space (Shine and Sinha 1991; Spencer and Braswell 1997; Colman 2001).

The warm pool region over the tropical western Pacific Ocean is thought to be the heat engine of the entire globe because it releases huge amount of latent heat from deep convection and plays an important role in driving the global atmospheric circulation and heat transport (McPhaden 1999).

1.1.2 Importance of organized features

Of the various modes of tropical organized convection, the Madden-Julian Oscillation (MJO) is one of the most critical. It dominates tropical variability on sub-seasonal timescales and is known to have global influences through tropical-extratropical interactions (Lawrence and Webster 2002). The MJO was discovered by Madden and Julian (1972a) and may be defined as an eastward propagating global scale atmospheric disturbance in the equatorial region with an intra-seasonal (30-90 days) periodicity. The active phase of MJO often provides the environment for high impact

weather events such as tropical cyclones and monsoon precipitation anomalies and there is increasing evidence that surface wind forcing from the MJO may play a crucial role in the initiation and amplification of El Nino (Madden and Julian 1994; McPhaden 1999).

The inability to predict large-scale organized convective systems in the tropics literally translate to larger numbers of weather fatalities and property damage than would occur in the absence of these forecast failures. These forecast failures are not just limited to short-term failures in the prediction of conditions in the tropics and subtropics as the distribution of organized, large-scale deep convection in the lower latitudes degrades weather prediction in the higher latitudes through tropical cyclones and other processes that produce high-impact weather in mid latitudes. Uncertainties such as the degree and manner of organized convection are influenced by and feedback onto the large scale atmospheric circulation. The fundamental mechanism that drives tropical atmospheric variability constitutes significant impact on weather and climate.

1.1.3. Representation of convection in numerical weather prediction

Deep convective storm development is arguably one of the most fundamental errors in models used for weather and climate prediction and its representation remains one of the most challenging problems facing meteorologists (Arakawa, 2004).

Cumulus convection, represented by convective parameterization, plays a central role in numerical modelling of the atmosphere. Convective parameterization is defined as formulating the statistical effects of moist convection to obtain a closed system for predicting weather and climate.

It has been recognized for many years that the parameterization of the major physical processes related to deep tropical convection is critical in global circulation models (GCMs). Several studies have shown the deficiencies in GCMs in simulating the multi-scale organized convection in the tropics. Examples are the poor representation of the MJO and other modes of tropical variability (Lin et al. 2006); the incorrect representation of the frequency of occurrence of high and low intensity rainfall events (Sun et al. 2006);

the poor representation of the diurnal cycle of rainfall (Betts and Jakob 2002). Many of these shortcomings are ascribed to the poor representation of sub-grid-scale processes in particular that of cumulus convection.

Classical convection theory emphasizes the temperature and humidity of the boundary layer and the temperature of the free tropospheric environment (the atmospheric instability as measured by the convective available potential energy [CAPE]) within which convective clouds may develop. However, the relationship between CAPE and convection is not as straightforward as often claimed. Sherwood (1999) for instance, found that there is enough CAPE for convection in the tropical western Pacific for 90% of the time but only 20-30% is likely to materialized into convective activities; other factors appear to play a role. Arakawa (2004) pointed out that we are missing most of the interaction involving multiple interaction processes as the current modeling efforts have been spent mainly on coupling each physical process with the dynamics core more or less independently from the others. He highlighted that all surviving convective parameterization schemes can be interpreted as adjustment schemes and concluded that the main task of convective parameterization is to provide a negative feedback by adjusting the temperature lapse rate in the tropical troposphere to realistic values. He further concluded that at least in the tropics, planetary boundary layer processes (PBL) are crucial in regulating moist convection above. Particularly over land, PBL processes associated with diurnal change must be considered in determining convective activities above.

Convective parameterizations used in GCMs generally only simulate the mean or the 1st-order moment of convective ensembles and do not explicitly include higher-order moments (e.g. variance). Lin and Neelin (2000) suggested a stochastic convective parameterization which will represent higher-order moments associated with convection appears to be able to simulate at least a part of the total convective variance that is often underestimated by GCMs. They further revealed that not only variance amplitude is important in parameterizing unresolved second moment effects, but that autocorrelation time is also important. Longer timescale unresolved mesoscale motions may be important to explicitly include in convective parameterizations and that relatively

short timescale noise (1 day or less) can affect tropical variability at longer, intra-seasonal timescales. They suggested that it will be useful for GCMs to explicitly include higher-order moments into the parameterization of sub-grid processes. It was emphasized in Arakawa (2004) that the trend in posing the convective parameterization is from deterministic and diagnostic closures to prognostic or stochastic closures and a statistical theory that governs the time evolution of the number of clouds is badly required.

1.2 Factors controlling tropical convection

The improper treatment of convection and how it couples with the large-scale flow translates into weaknesses in our ability to simulate sub-seasonal tropical variability, including the MJO and westerly wind bursts, which in turn make it difficult to simulate and predict the El Niño Southern Oscillation (ENSO) with coupled atmosphere-ocean models. Waliser et al. (1999) stated that an improved prediction of a prevalent MJO event can extend the atmospheric predictability by up to 20 days.

In order to understand the tropical weather, it is essential to gain an insight into the factors that control the intensity and organization of convection. Several factors have been identified that seem necessary or at least favourable for organized convection, including buoyant instability, water vapour above the trade wind inversion, upper-level divergence, low level convergence or upward motion at some level and upper-level vorticity (Sherwood, 1999; Tompkins, 2001b).

Though certain variables are known to affect the probability of convection, the variables presumed to be important precursors to convection are highly correlated with one another. For example, upward motions will lead to positive anomalies in humidity, deep instability and low level mass and moisture convergences with various time lags leaving uncertain as to which among these factors are the true causes of any subsequent outbreak. It has also been pointed out in Moncrieff (1992) that it is important to distinguish between the factors necessary for convection to begin “the activation” and those determining its subsequent behaviour once it has started.

1.3 Role of moisture in controlling tropical convection

Many studies indicate that moist convection is sensitive to free-tropospheric water vapour, including observational analyses and studies using cloud system resolving models (Brown and Zhang 1997; Tompkins 2001b; Bretherton et al. 2004; Sherwood et al. 2004; Derbyshire et al. 2004). Redelsperger et al. (2002) examined the factors that control the height of tropical convection and found that mid-level inversions and dry air entrainment into clouds both limit the vertical extend of convection. Soden and Fu (1995) find that the frequency of deep convection is strongly correlated with changes in upper tropospheric humidity.

1.3.1 Relationships between tropospheric moisture (Column Water Vapour) and Tropical Precipitation

The primary focus of this project will be in investigating the relationship between column water vapour (CWV) and tropical precipitation. The atmospheric CWV computed from the vertically integrated specific humidity is generally used as an indication of the amount of moisture available in the atmosphere.

$$\begin{aligned} \text{CWV} &= \int (\text{specific humidity} / \text{mean acceleration due to gravity}) dp \\ &= \int (q/g) dp \quad \quad \quad [(\text{CWV in kgm}^{-2}), (\text{Pressure in Pa, } q \text{ in kg/kg})] \end{aligned} \quad (1.1)$$

Unit for CWV corresponds to mm for equation 1.1.

A number of studies examined the relation of precipitation to humidity and its vertical structure, and how this relationship depends on the time and space scales under consideration (Ushiyama et al. 1995; Yoneyama and Fujitani 1995; Brown and Zhang 1997; Sherwood 1999; Bretherton et al. 2004). A general conclusion from these studies is that preconditioning the atmosphere humidity is essential for the development of organized convective systems. Episodes of deep convection are followed by increases

in mid- to upper-tropospheric relative humidity, while a relatively moist low- to mid-troposphere helps initiate tropical deep convection.

Results from the analyses over various tropical locations have shown that moisture profiles at mid- to upper tropospheric levels play an important role in the vertical development of tropical convective clouds.

Yoneyama (2003) studied the characteristics of moisture variability over the tropical western Pacific warm pool region and demonstrated the frequent occurrences of high relative humidity centered around 945 hPa and 560 hPa. They stated that the variation of CWV is well represented by the synoptic scale mid-tropospheric moisture variation. Holloway and Neelin (2009) showed that the first vertical principal component of specific humidity is very highly correlated with CWV and has a maximum of both total and fractional variance captured in the lower free troposphere (around 800 hPa). They further concluded that moisture profiles conditionally averaged on precipitation indicate a strong association between rainfall and moisture variability in the free troposphere (850-200 hPa), but little association with boundary layer (surface-850 hPa) variability.

Zelinka and Hartmann (2009) concluded that intense precipitation events in the tropics are preceded by an increase in low level humidity, while the humidity increase at upper levels and associated decrease in clear-sky longwave emission persist for many hours after the convective event. They stated that convection removes water vapour from a very moist source (boundary layer) by condensing a portion into precipitation and by transporting a portion to the very dry upper troposphere, resulting in dramatic changes to the upper-level moisture. They found that greater upper-tropospheric moistening and cloudiness are associated with larger-scale and better-organized convective systems, but even weaker, more isolated systems produce sustained upper-level humidity and clear-sky outgoing long-wave radiation anomalies.

Several recent studies have illustrated an empirical relationship between tropical column water vapour, CWV and precipitation, including a sharp increase or pickup of conditionally averaged precipitation at sufficiently high CWV (Bretherton et al. 2004;

Peters and Neelin 2006, Holloway and Neelin, 2009). Peters and Neelin (2006) found that precipitation, conditionally averaged by CWV over many individual events, tends to increase slowly up to some critical value and then rapidly increase above that. Holloway and Neelin (2009) showed the sharp pickup in precipitation occurs near a critical value of CWV and stated that it is unlikely that the increase in water vapor is just a result of the falling precipitation.

Bretherton et al. (2004) found a tight exponential relationship for all tropical ocean regions and seasons between the monthly means of surface precipitation rate P and column-relative humidity r . They showed that the increased column-relative humidity at higher rainfall rates is due to a broad specific humidity increase between 400 and 850 hPa on daily time scales and that the precipitation-related humidity anomalies extend down to the surface for monthly time scales.

1.3.2 Representation of tropospheric moisture in convective parameterization

As stated in section 1.1.3, convective parameterization is one of the most challenging issues in GCMs; the ability to properly simulate deep convection and the corresponding cloud and humidity fields remains a challenge to numerical modelling. Since precipitation processes in climate models are very sensitive to the method of convective parameterization (Slingo et al. 1996), it is of interest to investigate the representation of tropospheric moisture and precipitation in convective parameterizations.

Derbyshire et al. (2004) evaluated the sensitivity of cumulus convection to humidity in the free troposphere using cloud-resolving models (CRMs) and made comparisons with single-column models (SCMs). They suggested that most of the differences between the CRMs seem to arise from either the condensation schemes or the microphysical differences such as the treatment of cold cloud used in the models. They indicate that shallow convection is more sensitive to resolution and boundary layer nudging relative to the deep convection regimes. The sub-grid turbulence scheme was shown not to be critical, at least for the deep convection cases. However, most of the convection schemes have limited ability in adapting their entrainment and detrainment to the environmental conditions. They further concluded that SCMs giving substantial humidity

adaptation in the mass fluxes matched more closely to the CRM results and greater adaptivity in updraught mixing models can give more credible humidity sensitivities.

Bretherton et al. (2004) emphasized that though the absolute calibration of the r - P relationship is somewhat dependent on the datasets used to derive r and especially P , the results nevertheless do provide a useful constraint on conceptual models and parameterizations of tropical deep convection. In particular, they stated that deep convective parameterizations that relax the humidity to a fixed reference profile (e.g., the Betts–Miller scheme, Betts (1986)) might perform better if the reference relative humidity profile were adjusted to be precipitation dependent. Also, these schemes should use a moisture adjustment time scale t_c of roughly 12 h which is much larger than the time scale of 1–2 h that has typically been used at horizontal grid-spacings on the order of 300 km.

Holloway and Neelin (2009) concluded that higher CWV results in progressively greater plume buoyancies for several mixing schemes, notably in upper-tropospheric buoyancy that can yield deep convection. Higher values of lower-tropospheric (850-400 hPa) humidity, via entrainment, play a major role in this buoyancy increase and a small but significant increase in sub-cloud layer (below 950 hPa) moisture with increasing CWV also contributes to buoyancy. Entraining plumes tend to be far more buoyant at middle and upper levels for profiles with larger CWV values. They stated further that constant mixing, similar to many convective parameterizations, must be rather small in order not to kill convection by the time it reaches the middle troposphere and suggested that the observational constraints on entrainment may be useful in revising GCM convective parameterizations.

Project aims

It has been demonstrated in a number of recent studies that moist convection over the tropical ocean is sensitive to free-tropospheric water vapour which is not well represented in numerical modelling. Bretherton et al. (2004) analyzed the relationship between water vapour path precipitation rate over four different tropical oceanic regions (the Indian Ocean, the west Pacific, the east Pacific and the Atlantic Ocean) with P and r estimated using the brightness temperature from remote sensing systems; Holloway

and Neelin (2009) presented their study based on five years of radiosonde and precipitation gauge data from the Nauru Atmospheric Radiation Measurement (ARM) site (0.5°S, 166.9°E).

Yang and Slingo (2001) indicate that diurnal cycle varies regionally due to the modulations of low level convergence by land/sea breezes, topography effects as well as mesoscale features and these modulations play a crucial role in the heat and moisture budget over the maritime continent. They concluded that oceanic deep convection tends to reach its maximum in the early morning, while continental convection typically peaks in the late afternoon and evening.

These studies motivate us to investigate the precipitation-RCWV relationship over tropical land.

A key goal of this study is to investigate the robustness in the relationship between column water vapour / relative column water vapour and precipitation rates over the tropical oceanic and land regions through observations and model simulations.

In the first part of this project, we

- Investigate the relationship between Relative Column Water Vapour (RCWV) and precipitation
- Examine the factors contributing to such relationship and
- Perform a precipitation lag-lead analysis

over Singapore (1.3°N, 103.9°E, within the maritime continent) in the western equatorial Pacific.

The second part of this project will focus on examining the relationship between the precipitation and CWV through a 30 day period' simulated data over the tropical Indian and West Pacific Oceans from Unified Model version7.1. Data of 40 km grid spacing will be contrasted with 12 km grid spacing simulated data. The interaction between moisture fields and precipitation will also be studied by analyzing the moisture budget for the 30 day period over the tropical Indian and West Pacific Oceans.

Chapter 2 outlines the data used to fulfill the first part of this project. Methodology and results of the analyses through observations and model simulations will be presented in chapter 3 and 4. Chapter 5 summarizes the results presented in the project along with limitations and potential areas of extension to the work conducted in this project.

Chapter 2 Data description and categorization

In the first part of this study, we analyse twelve years of radiosonde and precipitation gauge data from 1 Jan1996 – 31 Dec 2007 obtained from the Meteorological Services Division, National Environment Agency of Singapore. Daily radiosonde data (0000UTC, 8am local time & 1200UTC, 8pm local time) are used, with corresponding daily accumulated rainfall data from Changi station (the official station used for the computation of climatological conditions in Singapore). Note that the sonde data available only went up to around 500 hPa.

As a basic quality check, data with obvious retrieval errors (e.g. those with relative humidity greater than 100%) are discarded. Data are then further constrained to be within reasonable ranges by removing those which are of significant outliers from the norm. i.e. data greater than (median + 3/2*(inter-quartile range)) and less than the (median - 3/2*(inter-quartile range)) are removed. Inter-quartile range is defined as the difference between the 75th and the 25th percentiles.

In total, 8,675 sondes, 4,343 and 4,332 for 0000UTC & 1200UTC respectively have been retained for the analysis. The radiosonde data are then interpolated onto pressure intervals of 5hPa within 1005hPa – 530hPa.

Corresponding daily mean rainfall in mm/hr will be used in our analyses.

The atmospheric column water vapour (CWV), equation 1.1 as defined in section 1.3.1, computed from the vertically integrated specific humidity up to 530 hPa will be used here as an indication of the amount of moisture available in the atmosphere.

Relative Column Water Vapour (RCWV) is then calculated by taking the percentage ratio between CWV computed from specific humidity and saturated specific humidity.

$$\text{RCWV} = (\text{CWV} (q) / \text{CWV} (q_s)) * 100\%$$

Figure 1 shows the distribution of the data set, clustered into bins based on RCWV. The data are generally clustered into bins with $\text{RCWV} \leq 50\%$, $50\% < \text{RCWV} \leq 60\%$,

60%<RCWV≤70%, 70%<RCWV≤80% and RCWV>80%. The main feature to be highlighted from figure 1 is the limited number of data available in the first bin, which should be bare in mind when considering later figures. A large portion of the data lies between 60% < RCWV ≤100% with a peak in the 70% <RCWV≤80% bins at both 0000Z and 1200Z. These features agree generally with the distribution plot of observations shown in fig 3b of Bretherton et al. (2004); figure C1 in appendix C. It can be argued here that there is some diurnal effect in the distributions of the RCWV; the greater number of observations with RCWV≤70% and a smaller set of observations with RCWV>70% at 1200Z. A more detail discussion on this distribution will be done in sections 3.2 and 3.6.

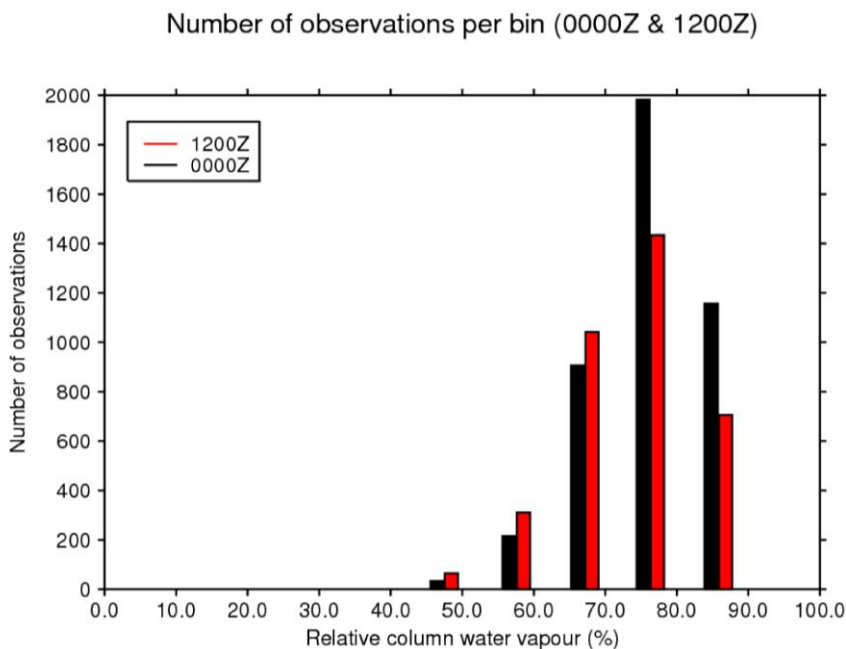


Figure 1: Number of observations in each bin

It is known that weather in the tropics is significantly affected by ENSO (El Nino, La Nina, and Neutral conditions) episodes and Monsoon seasons; we will also conduct our study by further categorizing the dataset according to Monsoons affecting Singapore and the ENSO episodes based on the Climate Diagnostics Center (CDC) statistics.

2.1 Climatology of Singapore

Climatologically, Singapore is characterized by small variations in temperature and pressure and high humidity and abundant rainfall throughout the year. The prevailing

wind over the region is largely influenced by the belts of high pressure centered near latitude 30° N and 30° S and an equatorial trough of relatively low pressure lying between these two high pressures.

The climate over Singapore can be divided into two main monsoon seasons, the Northeast monsoon season (December – March) and the Southwest monsoon season (June - September). Separating these two monsoon seasons are two relatively short inter-monsoon periods (April – May and October – November).

Although there are no marked wet and dry periods, the mean monthly rainfall shows drier weather conditions from May to July and wetter conditions in the months of November to January. The Northeast monsoon season can be divided into a relatively wet phase and a dry phase. The wet phase of the Northeast monsoon season occurs in December and January while the later part of the Northeast monsoon season (late January and February) is in the dry phase where days are generally fair and occasionally windy with little or no rain. Predawn to midday squall lines are common in the Southwest monsoon. Showers/thunderstorms generally occur in the afternoon and early evening during inter-monsoon periods. (Source: Meteorological Services Division, National Environment Agency of Singapore; http://app2.nea.gov.sg/topics_met.aspx)

Figure 2 shows a schematic diagram of monsoons affecting Singapore.

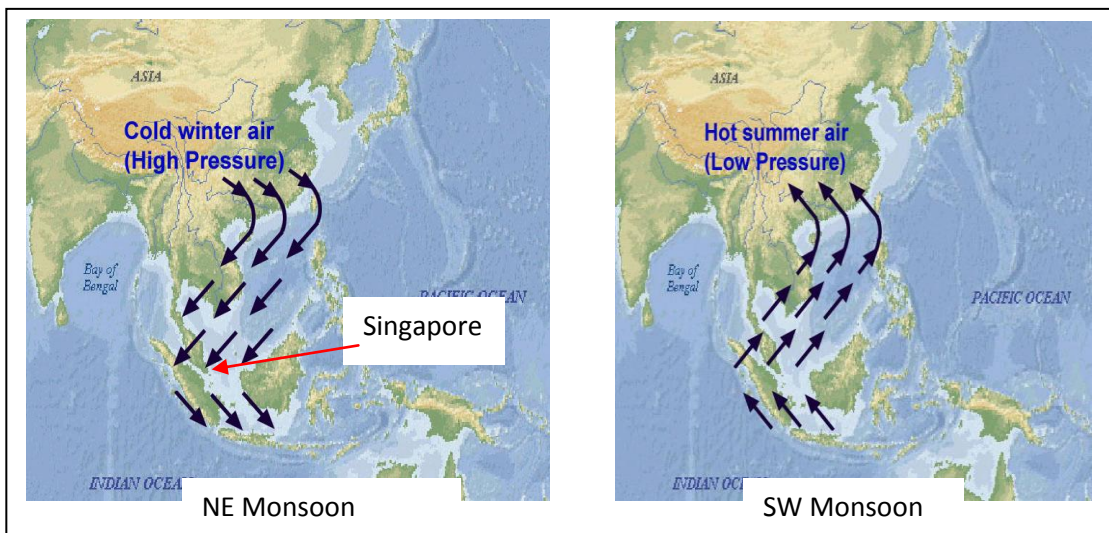


Figure 2: Monsoons affecting Singapore
Source of map: www.world-maps.co.uk

2.2 Distribution of data set

The distribution of the RCWV data set for monsoons and ENSO episodes is shown in figures 3 and 4 respectively. In terms of Monsoons, data are divided into Wet NE monsoon (January and December); dry NE monsoon (February) and March, with generic NE prevailing winds; the transition between NE to SW monsoon (April and May); the SW monsoon (June - September) and the transition between SW to NE monsoon (October and November). Four El Nino episodes and two La Nina episodes (including the strong El Nino in 1997-1998 and the strong La Nina in 1998-2000) are considered in our analysis period.

Note that the El Nino and La Nina episodes are further categorized according to their intensities (i.e. weak, moderate & strong) based on the CDC definition. El Nino and La Nina are taken to be the total of these sub-cases. The data are clustered into the same bins as in figure 1. We find a similar number of observations in the $70\% < RCWV \leq 80\%$ and $RCWV > 80\%$ bins during the wet NE monsoon seasons (figure 3). Plausible contributing factor to such departure in distribution will be discussed in section 3.5. An increase in the number of observations from the $70\% < RCWV \leq 80\%$ bin to the $RCWV > 80\%$ bin during the La Nina episode is being observed in figure 4. There is obviously a limited number of observations available in some of the sub-divisions, particularly for the Feb, March, weak El Nino and the moderate La Nina cases.

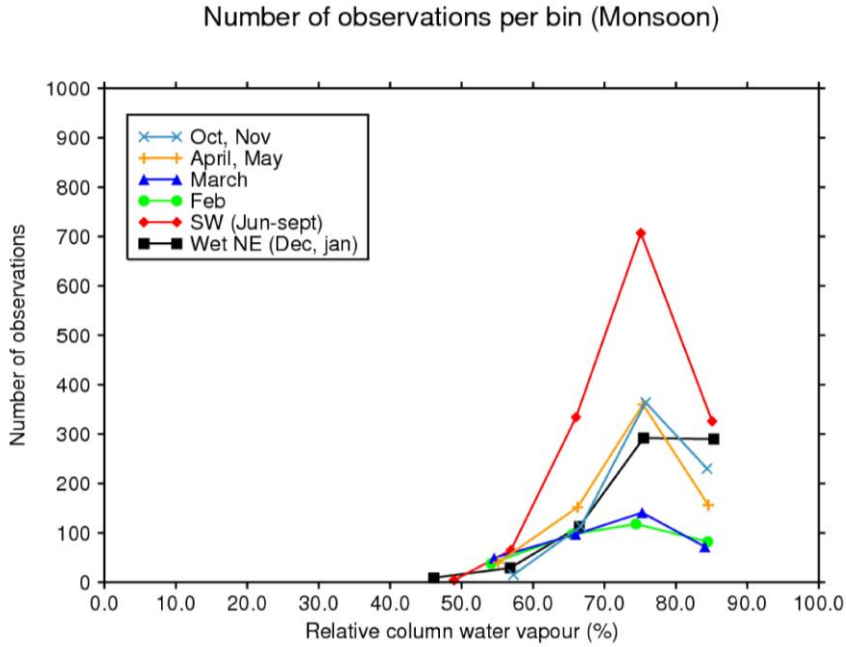


Figure 3: Number of observations in each bin (Categorized based on Monsoons)

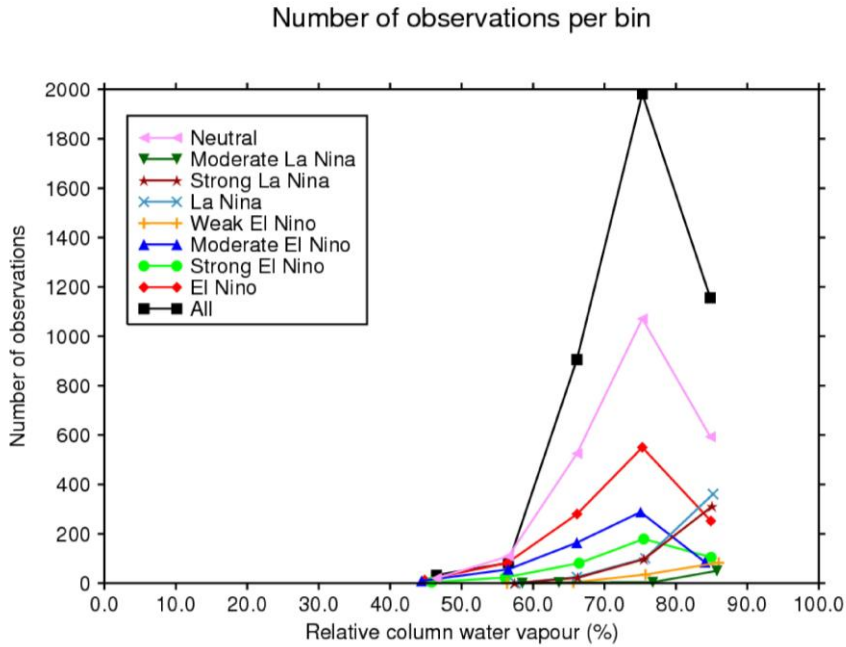


Figure 4: Number of observations in each bin (Categorized based on ENSO episodes)

Chapter 3 Results I: Relationships between Relative Column Water Vapour and Tropical Precipitation (Sonde Observations)

3.1 Effect of precipitation on moisture structure

Figures 5 and 6 compare the vertical profiles of relative humidity, R.H. and the specific humidity, q conditioned on daily mean rainfall respectively. The three higher precipitation categories (daily mean rainfall ≥ 1 mm; green, yellow & red curves in figure 5) correspond to nearly uniform moistening between the surface and 530 hPa, i.e. they correspond to profiles with little vertical gradient from profiles with lower precipitation. The most striking feature of these profiles is the large spread of R.H. in the free troposphere (850hPa – 530hPa). It is the free tropospheric moisture rather than the boundary layer (below 950 hPa) moisture that increases with increasing rainfall.

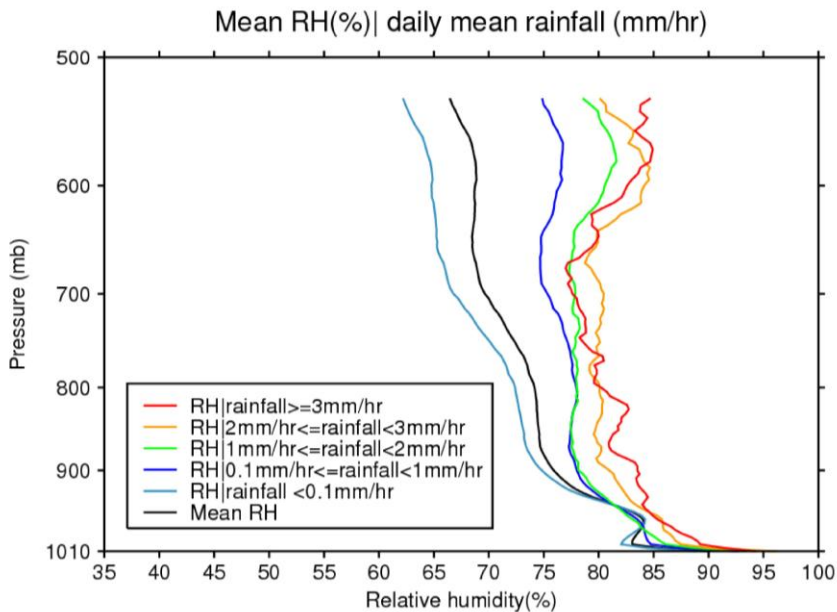


Figure 5: Relative humidity (%) profiles at 0000Z conditioned on daily mean rainfall (mm/hr). A similar trend can be obtained from 1200Z profiles (not shown here)

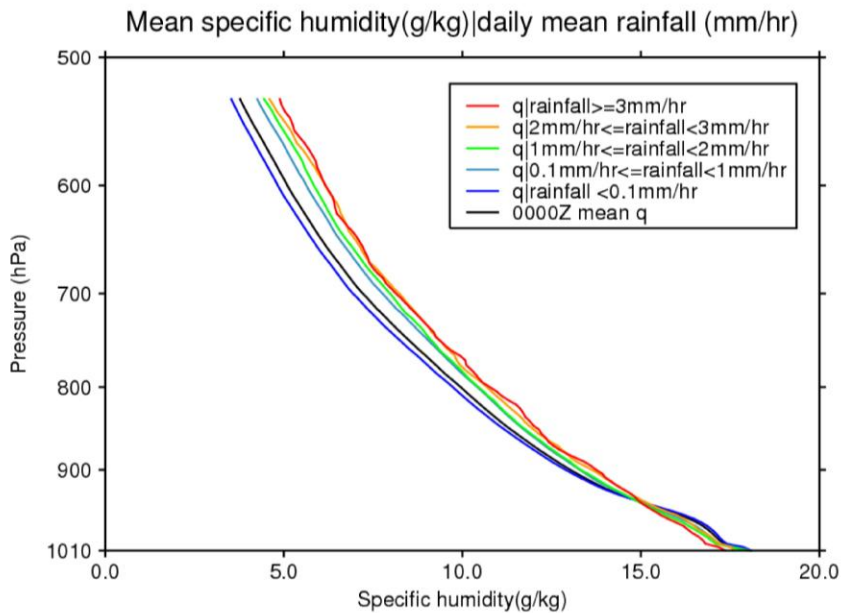


Figure 6: Specific humidity (g/kg) profiles at 0000Z conditioned on daily mean rainfall (mm/hr). A similar trend can be obtained from 1200Z profiles (not shown here)

Specific humidity profiles conditionally averaged on precipitation (figure 6) also show a strong association between rainfall and moisture in the free troposphere, and little boundary layer variability. These results are consistent with the analyses of Bretherton et al. (2004, their figure 9; figure C2 in appendix C); Holloway and Neelin, (2009, their figure 1; figure C3 in appendix C). Another feature to highlight here is the transition from lower moisture contents in the boundary layer (below ~950 hPa) to higher moisture contents above the boundary layer during the wet periods. This transition in moisture contents might be attributed to the transport of moisture from the boundary layer to the free troposphere or also, could be drying from downdrafts by convection.

3.2 Rainfall intensity conditioned on Column Water vapour and Relative Column Water Vapour

The relationship between daily mean rainfall conditioned on CWV (Figure 7) shows a sharp pickup of precipitation above approximately 48mm in CWV, an increment of precipitation rate of 1.9mm/hr (0.1mm/hr to 2.0mm/hr) correspond to an increment of 1mm in CWV (around 47.8mm to 48.8mm). This sharp pickup in precipitation above critical CWV agrees with the results concluded from other studies (Bretherton et al.

2004 [their fig 2a; figure C4 in appendix C]; Holloway and Neelin 2009 [their fig 3b; figure C5 in appendix C]).

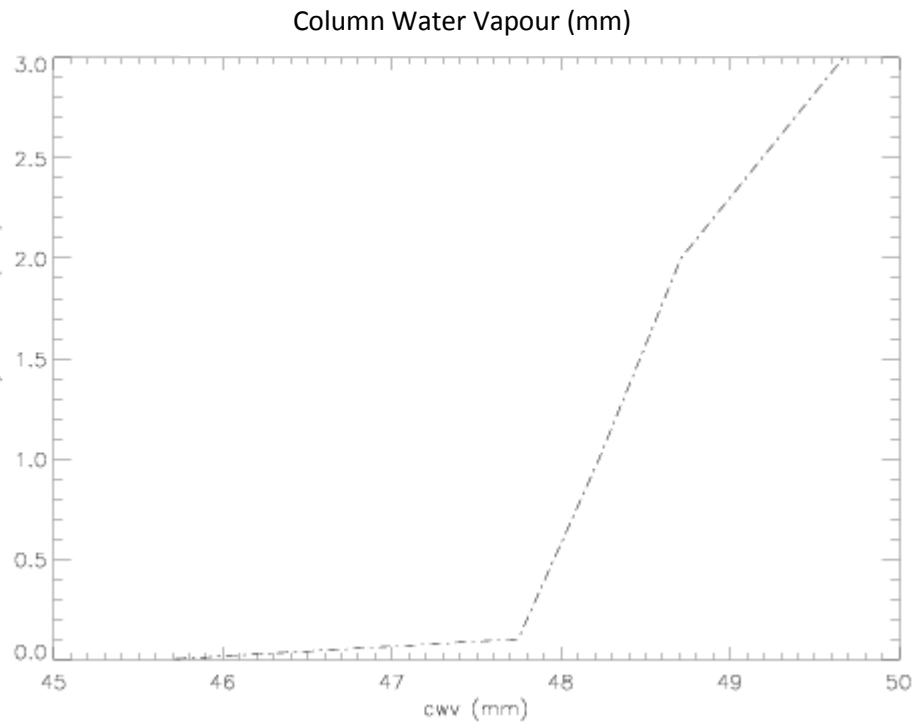


Figure 7: Daily mean rainfall (mm/hr) conditioned on column water vapour (mm)
y-axis: rainfall in mm/hr; x-axis: CWV in mm

3.2.1 Daily mean rainfall conditioned on Relative Column Water Vapour (ENSO and Monsoons categorization)

Motivated by Bretherton et al. (2004) in the usage of column averaged relative humidity (r in their context) in place of CWV (the underlying aim was to remove the regional differences in the water vapour path versus precipitation relationship); daily mean rainfall conditionally on relative column water vapour (RCWV) will be considered in our discussions here.

The relation between daily mean rainfall conditioned on RCWV based on the total observations and on Monsoons categorization is shown in figure 8. The first general conclusion is that of the steady increasing trend in precipitation shown in figure 7 is again a striking feature in figure 8. It thus provides more confidence in this important

steady increasing trend between precipitation intensities and atmospheric moisture content.

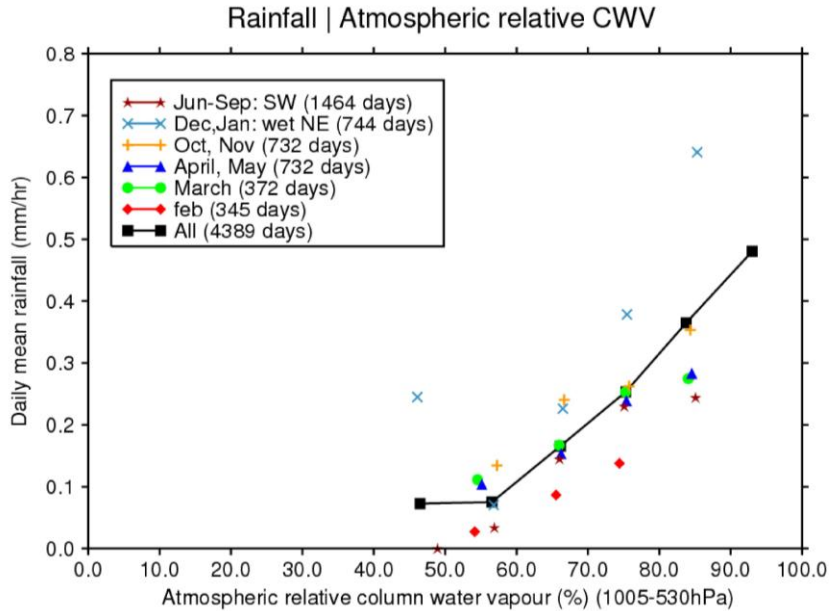


Figure 8: Daily mean rainfall (mm/hr) conditioned on relative column water vapour (%) based on total observations and monsoons.

Another feature to be highlighted from this plot is that the steady increase of rainfall intensity above a sufficiently high RCWV is common to all monsoon seasons. As mentioned in chapter 2, the data point for $RCWV \leq 50\%$ (the 1st bin) has to be down-weighted due the limited number of observations available. Note that the overall data is further categorized to include a $RCWV > 90\%$ bin. It should be emphasized here that there is no observation with $RCWV > 80\%$ for the dry NE monsoon period (Feb), which again highlights the close relationship between precipitation and RCWV.

It can further be concluded that the relationship shown for Wet NE monsoon (pale blue cross) agrees best with the fit shown in figure 3a of Bretherton et al. (2004); figure C6 in appendix C. Note that the RCWV presented in this study corresponds to the r in Bretherton et al. (2004) but is measured only up to 530hPa. This suggests the possibility of the effect of moisture advection from the ocean (the South China Sea) in generating a heavier precipitation with the same RCWV which will be discussed in section 3.5.

Daily mean rainfall conditioned on RCWV and categorized according to ENSO episodes is shown in figure 9a. The conclusion of the steady increase in rainfall intensity above a sufficiently high RCWV can again be identified from the plot. It is to be pointed out here that the limitation of data availability may contribute to the scatter in the strong El Nino episode (purple circles) and the decrease in precipitation from the $70\% < RCWV \leq 80\%$ to $RCWV > 80\%$ bins during La Nina episodes (dark blue cross).

In order to investigate the vertical profiles and the relative importance of the lower-tropospheric (850-550hPa) and boundary layer (1005-950hPa) moisture associated with the transition to high precipitation, we will next consider the relationship of rainfall intensity conditioned on the total tropospheric, the lower-tropospheric and boundary layer RCWV.

It is clear from figures 9a and 9b that the steady increase in the daily mean rainfall intensity above a threshold RCWV occurs when conditioned on the total or on the lower tropospheric relative column water vapour. Also, the relationship is robust regardless of ENSO episodes.

There is, however, no very clear correlation exhibited between precipitation rates and boundary layer RCWV (Figure 9c). Although on an average over all observations, we do still notice a slight positive correlation, the steady increasing trend in precipitation is not well exhibited here. (Similar conclusions can be argued based on Monsoon seasons, not shown here.)

These analyses suggest that moisture above the boundary layer is the key component in the relationship between RCWV and the transition to deep convection and higher average precipitation rates. These results are consistent with the analyses of Holloway and Neelin (2009), supporting their concluding statement on the key role of lower tropospheric moisture in the transition from shallow to deep convection.

Rainfall conditioned on total relative CWV (ENSO)

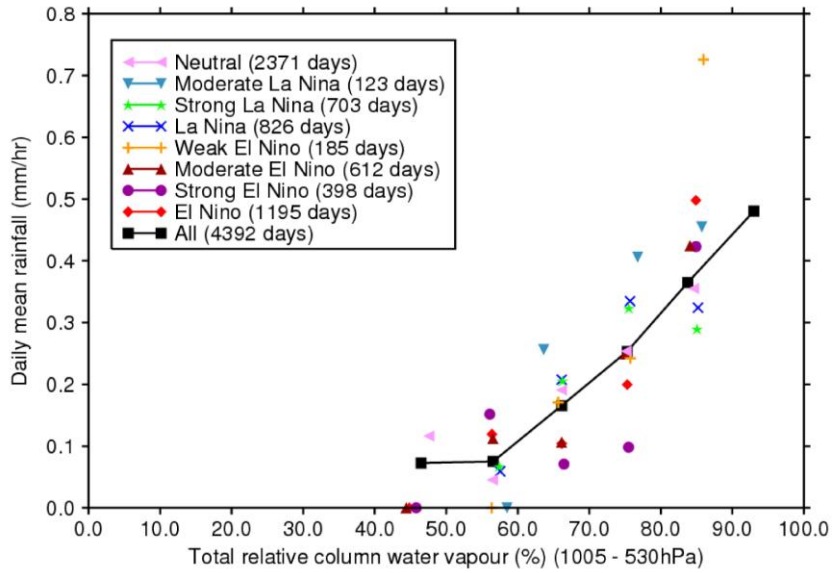


Figure 9a

Rainfall conditioned on lower tropospheric relative CWV (ENSO)

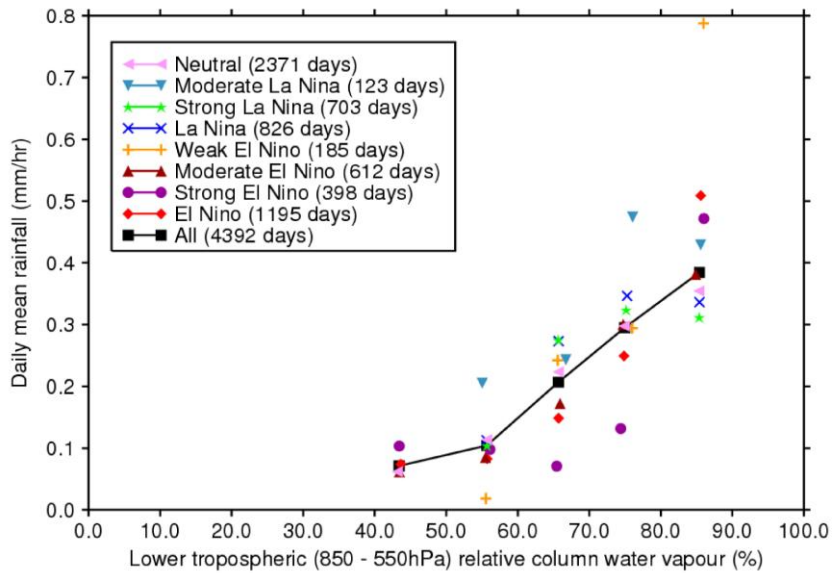


Figure 9b

Rainfall conditioned on boundary layer relative CWV (ENSO)

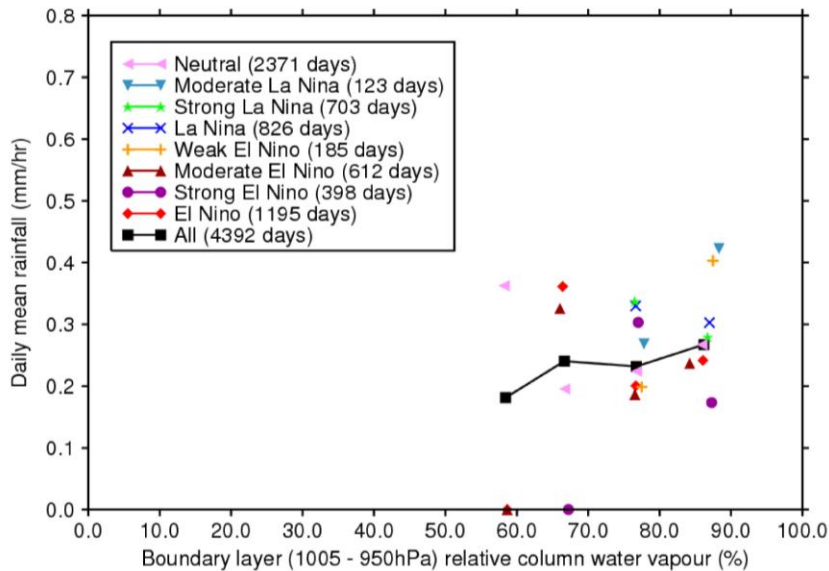


Figure 9c

Figures 9a, 9b and 9c: Daily mean rainfall (mm/hr) conditioned on total, low-tropospheric (850-550hPa) and boundary layer (1005-950hPa) relative column water vapour (%) respectively.

Further analysis in the precipitation-RCWV relationship for data classified based on ENSO episodes within monsoon seasons which indicate some departures from the usual steady increment relationship are presented in appendix A.

To better look at possible physical mechanisms in contributing to the relationship between RCWV and precipitation, we will next turn our attention to analysing the effects of atmospheric temperature and wind structures in determining this relationship.

3.3 Impact of temperature on moisture structure

The diurnal cycle of moist convection is of major importance for weather and climate studies due to its strong radiative feedbacks, the resulting precipitation and its control on surface temperature. It is well known that in most of the tropics over land, the temperature conditions are almost entirely dominated by the diurnal cycle with short-term temperature variations almost always related to thunderstorms. Climatologically,

the diurnal temperature range over Singapore is around 7°C (24 °C - 31 °C) and it is common to observe a drop of up to 7°C within half an hour in a thunderstorm environment. (Meteorological Services Division, National Environment Agency of Singapore; http://app2.nea.gov.sg/topics_met.aspx)

In general, a locally developed deep convective cycle will begin with clear-sky boundary layer convection in the morning, followed by relatively shallow non-precipitating clouds and the onset of deep convection a few hours later. Clouds will tend to form where the surface heating (and evaporation) is strongest. One might thus hypothesize that there maybe an impact on the relationship between the rainfall rate and the atmospheric moisture content due to diurnal variation in RCWV.

This hypothesis will be discussed here. Table 3.1 shows that the difference between the means of RCWV at 0000Z and 1200Z is much smaller than the standard deviations evaluated at both 0000Z and 1200Z. These indicate that the variations in the mean diurnal RCWV will not have large impact on the precipitation-RCWV relationship.

Standard deviation in RCWV		Mean RCWV (0000Z) – Mean RCWV (1200Z)
0000Z	1200Z	
8.69221 %	9.45797 %	2.7881 %

Table 3.1: Standard deviations and differences between means of RCWV (%) calculated based on 0000Z and 1200Z profiles

Another point to note from table 3.1 is the larger standard deviation in the 1200Z relative to that in the 0000Z observations. This diurnal variation in RCWV will be discussed further in section 3.6.

The atmospheric temperature variations in Monsoons and ENSO episodes will next be considered. It is clear from figure 10 that there is only a small and almost constant, variation with height in the mean atmospheric temperature throughout the lower troposphere, within the range [-0.5K, 0.5K] over the ENSO episodes. The mean temperature during neutral conditions agrees closely with that of the overall mean

temperature profile. Mean temperature profiles during moderate and strong El Nino episodes are warmer than that of Neutral conditions, while La Nina is cooler relative to Neutral.

Figure 11 shows that the annual cycle of temperature variation is strongest in the boundary layer. The mean boundary layer temperature during the NE monsoon is lower than that of SW monsoon but this reverses above ~700hPa.

An obvious seasonal temperature cycle is observed over the monsoons in the boundary layer, which is coolest in the NE monsoon and warmest in April and May (the inter-monsoon), then decreasing gradually over the months to NE monsoon again. The results here indicate a larger diurnal temperature cycle relative to seasonal cycle [(7K diurnally; based on the guide to Singapore’s weather by meteorological services of Singapore; http://app2.nea.gov.sg/topics_met.aspx) to 2K seasonally shown here. Although only slight variations in temperature among seasons are observed, it might provide a potential explanation for the behaviour of the RCWV-precipitation relationship. We will thus consider the relationship between rainfall intensity and RCWV categorized based on vertically averaged tropospheric temperature (from 530 to 1005 hPa) next.

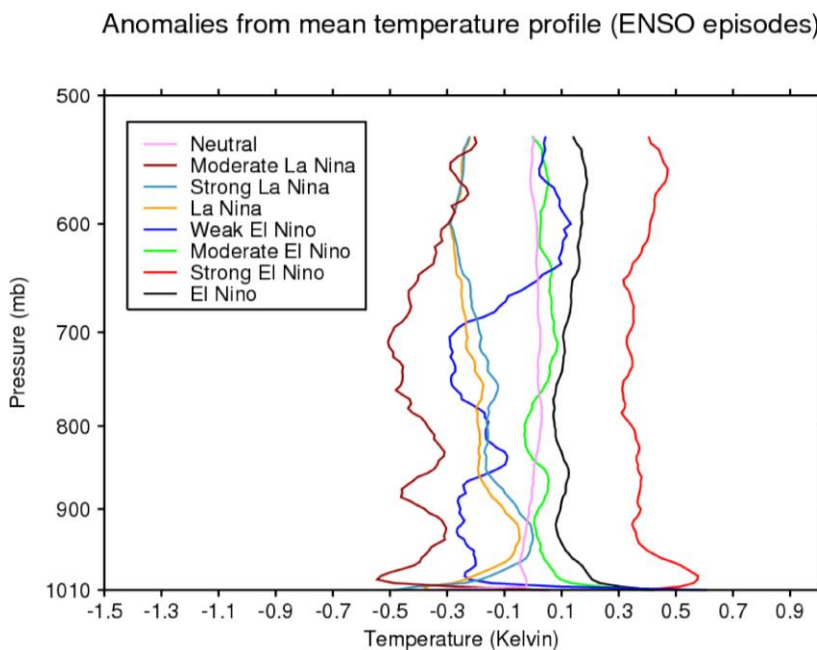


Figure 10: Tropospheric temperature (K) anomaly from the mean temperature profile.
ENSO

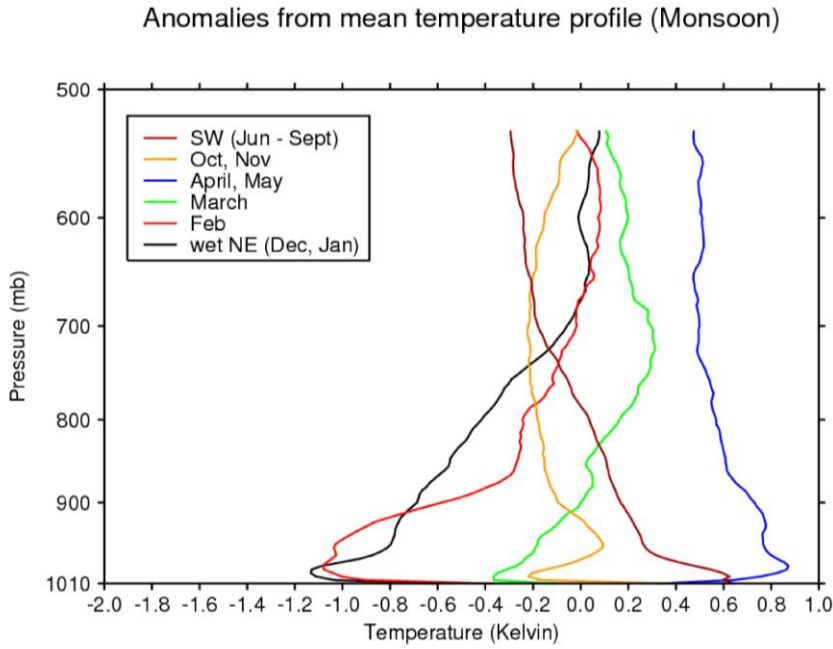


Figure 11: Tropospheric temperature (K) anomaly from mean temperature profile.
Monsoon

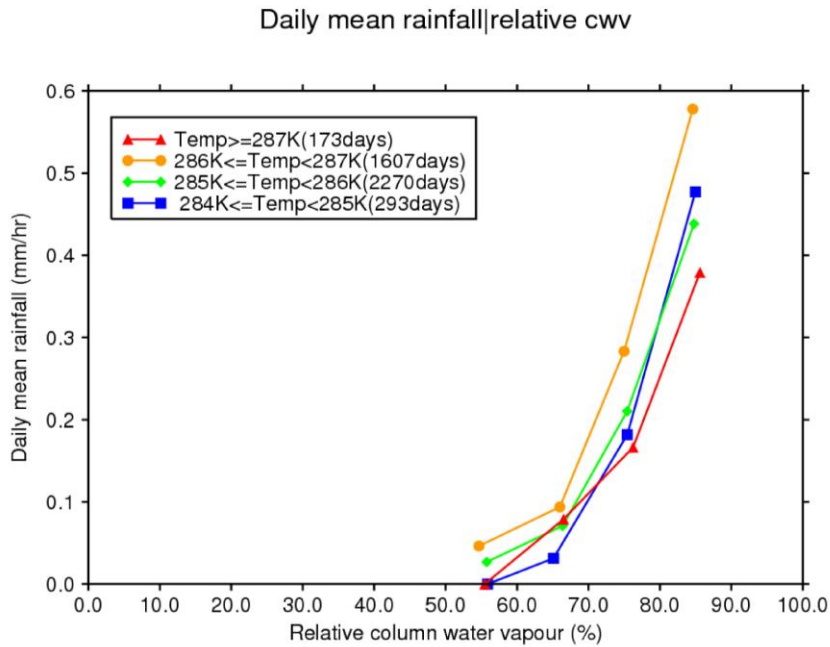


Figure 12: Daily mean rainfall (mm/hr) conditioned on RCWV (%) categorized according to atmospheric mean temperature (K)

It can clearly be identified from figure 12 that the variation in atmospheric temperature is unlikely to be a potential factor in influencing the relationship between RCWV and precipitation. The steady increasing trend in precipitation is robust in all temperature regimes.

Figure 13 provides us the distribution plot of observation per bin; data clustered according to the mean atmospheric temperature. They follow closely the distribution shown in figure 1 with a peak in the 70% <RCWV≤ 80% bin, majority of the days fall into the 285K to 287K categories.

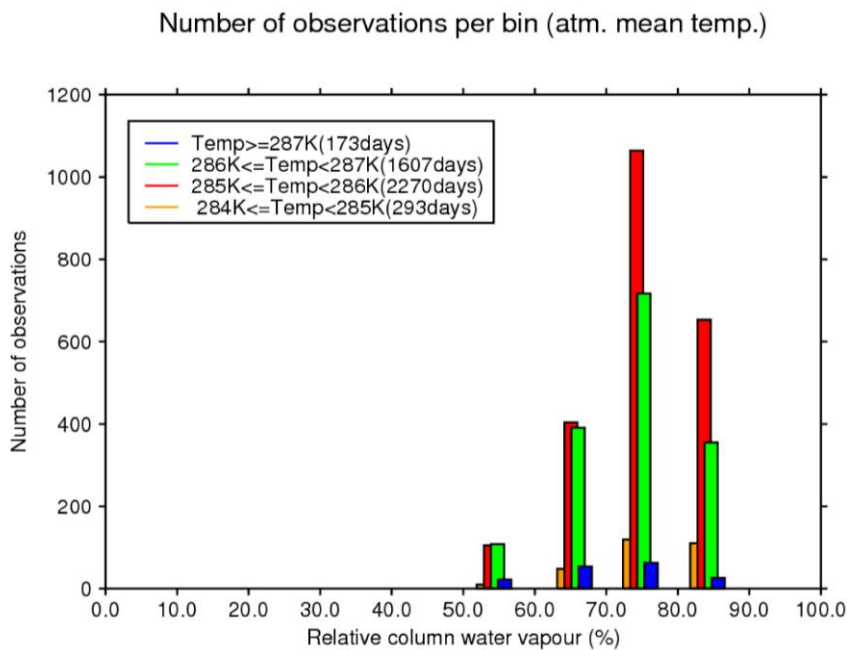


Figure 13: Number of observations per bin categorized according to vertically average tropospheric temperature (K)

The analyses discussed thus far focus on indicating the relationship between the mean precipitation intensity and RCWV; we will next move on to examine the distribution of the rainfall within each RCWV bin. Details such as the minimum, median, maximum, the 10th, 25th, 75th and 90th percentiles of the daily mean precipitation will be studied.

3.4 Daily mean rainfall range per bin

It has been shown in the previous section that the steady increasing trend in precipitation-RCWV relationship holds for both the 0000Z and 1200Z data. We will present here the analysis for the distribution of the daily mean rainfall per bin based on the 0000Z data, a similar relationship can be obtained from the 1200Z data.

As shown in figures 14a - 14e, the median hourly rainfall for all bins is zero (except for the bin with $RCWV \geq 80\%$ in the wet NE monsoon season, figure 14d). This indicates that high RCWV is a necessary but not a sufficient condition for strong precipitation, RCWV being one of the many factors that can influence the development and intensity of precipitation.

Three main features are highlighted from these plots:

- 1) The daily mean rainfall intensity falls around the 75th percentile of all bins with $RCWV \geq 60\%$. This result suggests that the precipitation-RCWV relationship obtained is likely to be dominated by the relatively small number of high precipitation events.
- 2) There is little difference in the 90th percentile of the precipitation intensity between bins of $70\% < RCWV \leq 80\%$ and $RCWV > 80\%$ (except for the wet NE monsoon case in figure 14d).
- 3) Another interesting observation from these plots is the maximum precipitation corresponds to the $70\% < RCWV \leq 80\%$ bin is generally larger than that corresponds to the bin with $RCWV > 80\%$ (again with exception for the wet NE monsoon). This indicate that extremely strong precipitation events need not necessary correspond to the highest RCWV bin.

Rainfall conditioned on total relative CWV (All 0000UTC)

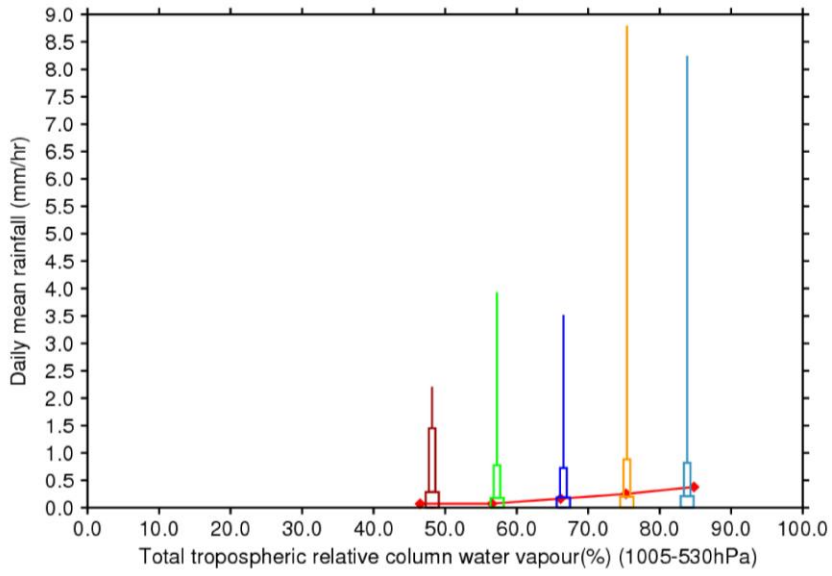


Figure 14a

Rainfall conditioned on total relative CWV (El Nino, 0000UTC)

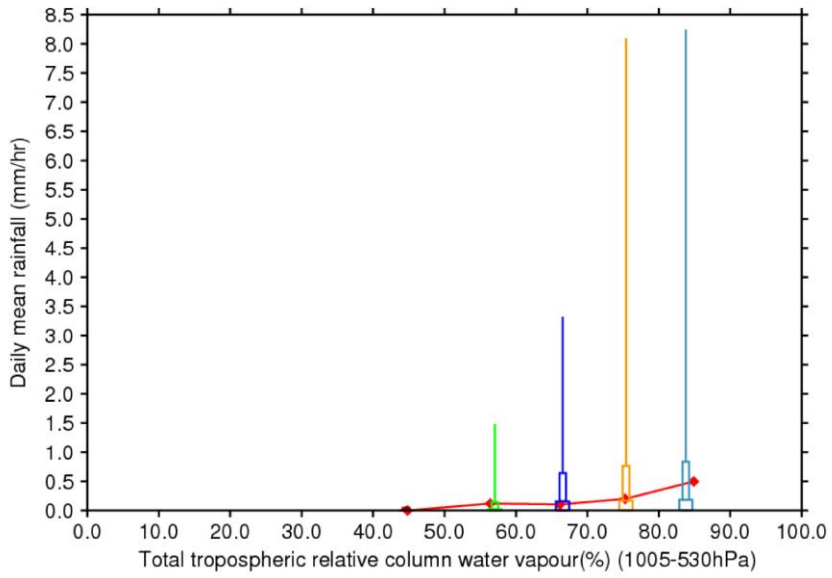


Figure 14b

Rainfall conditioned on total relative CWV (Neutral condition,0000UTC)

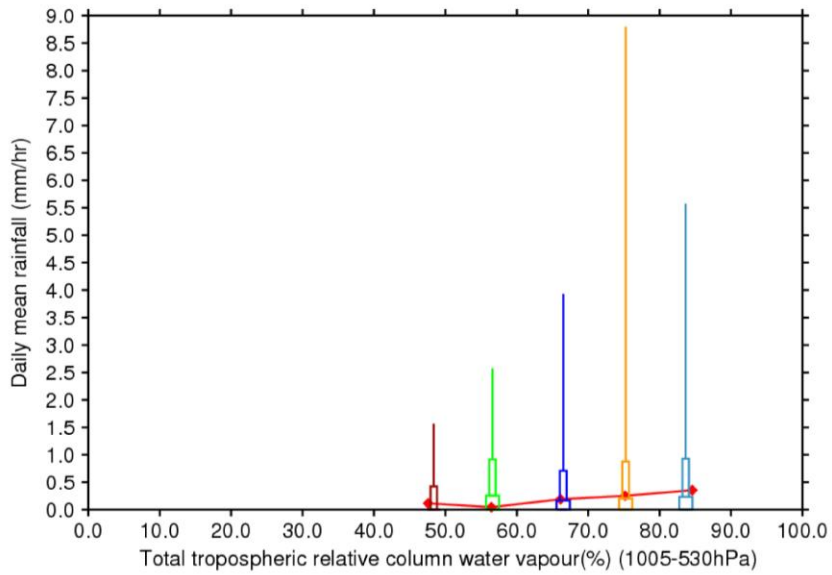


Figure 14c

Rainfall conditioned on total relative CWV (Wet NE:Dec, Jan)

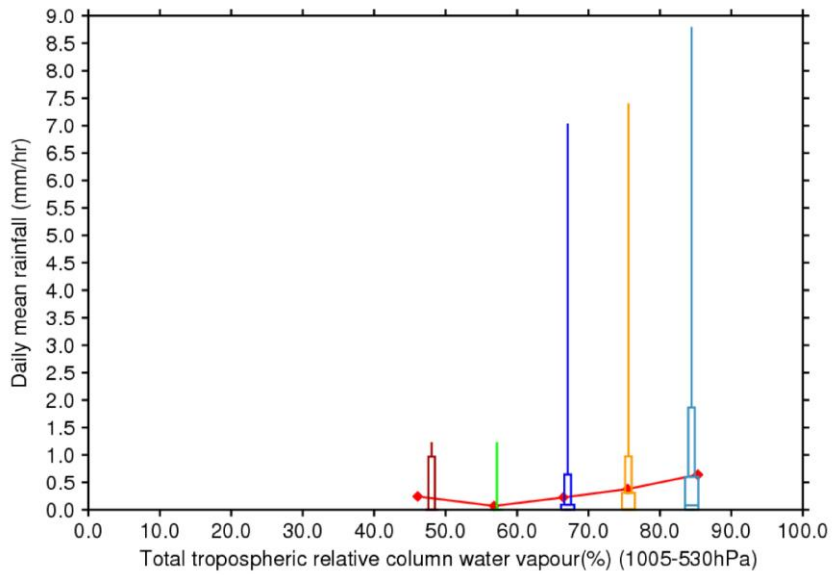


Figure 14d

Rainfall conditioned on total relative CWV (SW Monsoon:Jun-Sept)

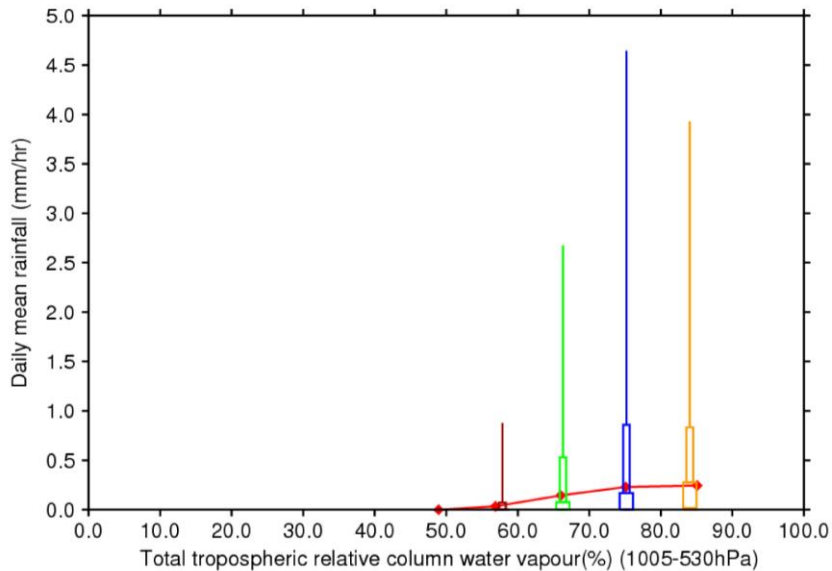


Figure 14e

Figures 14a – 14e: Daily mean rainfall (min, 10%, 25%, median, 75%, 90% & max (in mm/hr)) conditioned on the atmospheric RCWV (%). 14a) All observations; 14b) El Nino episodes; 14c) Neutral conditions; 14d) Wet NE monsoon & 14e) SW monsoon. The solid red line is the daily mean rainfall. (Similar results can be concluded in La Nina episodes and other monsoon seasons; not shown here)

3.5 Advection of moisture

As stated in section 3.4, wet NE monsoon is the only season which exhibits an increase in the 90th percentile precipitation intensity from the 70% < RCWV ≤ 80% bin to RCWV ≥ 80% bin. It is also the only season in which the maximum precipitation falls in the highest RCWV bin, the RCWV ≥ 80% bin. A natural follow up is to determine the contributing factors to this observed variation in characteristics between wet NE monsoons from others. Advection of moisture and thus enhancing the possibility of heavier precipitation is identified as a potential contributing factor to this feature.

To understand the impacts of the moisture source in the relationship between rainfall intensity and RCWV, the data is organized into six sectors based on geographical orientation and assumptions made on moisture source (Table 3.2). They are

categorized with the underlying aim of verifying the conjecture that high moisture contents will be advected from South China Sea for data in the 0° to 70° sector while relatively lower amount of moisture contents will be advected from the 160° to 260° sector associated with a shorter sea track. (The geographical location of Singapore is shown in figure 2).

It has been found that the total moisture variation on synoptic scales is well represented by the mid-tropospheric moisture variation (Yoneyama, 2003) and results from Holloway and Neelin (2009) indicate that variation in moisture is largest around 800mb. The wind conditions, based on the wind speed at 800mb will thus be used to verify the hypothesis that advected rather than local source of moisture may produce a modification of the relationship between rainfall intensity and RCWV. With the mean wind speed of 5.2m/s at 800mb, data are grouped based on wind speed $\leq 5\text{m/s}$ and wind speed $>5\text{m/s}$ within each sector.

Relative column water vapour is calculated based on this categorization and again clustered into bins with $\text{RCWV} \leq 50\%$, $50\% < \text{RCWV} \leq 60\%$, $60\% < \text{RCWV} \leq 70\%$, $70\% < \text{RCWV} \leq 80\%$ and $\text{RCWV} > 80\%$.

Sector	Assumed moisture source
0° to 20°	From South China Sea; partly modified along the track through southern Peninsula Malaysia
20° to 70°	From South China Sea (long sea track from the NE)
70° to 160°	From Java Sea and Borneo; relatively shorter sea track
160° to 260°	Mainly from Sumatra with slight modification along the short sea track over strait of Malacca
260° to 330°	Mainly from the strait of Malacca
330° to 360°	From the Peninsula Malaysia

Table 3.2: Sectors categorization and underlying assumption on moisture source

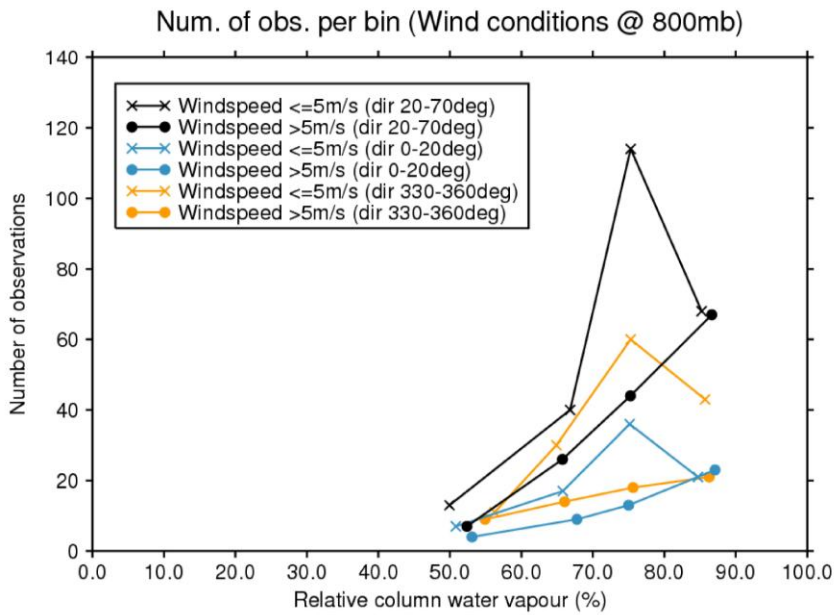


Figure 15a

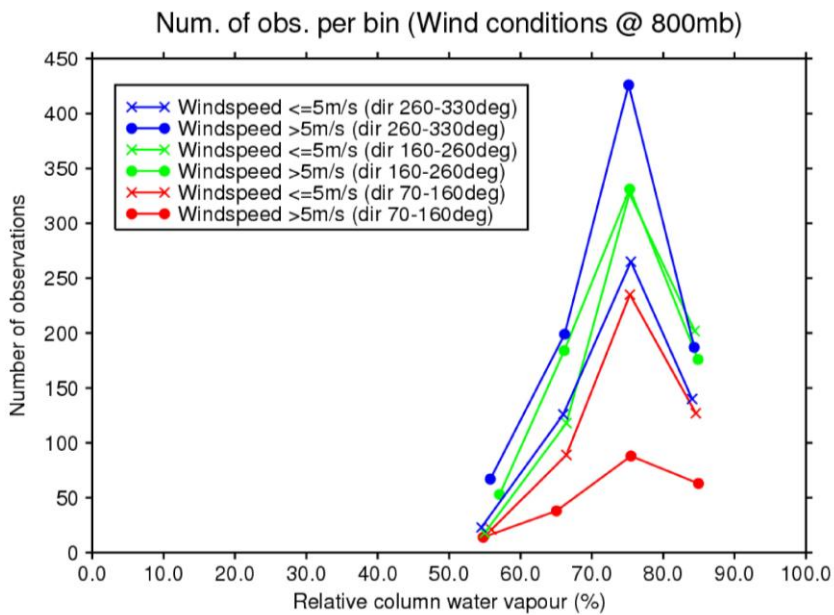


Figure 15b

Figures 15a and 15b: Number of observations in each bin in the six wind sectors
 18a: 330° - 70° (yellow: 330-360; pale blue: 0-20; black: 20-70)
 18b: 70° - 330° (red: 70-160; green: 160-260; dark blue: 260-330)
 'cross': wind speed ≤ 5m/s; 'circle': wind speed >5m/s

Figures 15a and 15b show the distribution of RCWV. Similar to figure 1, we have limited observations for the bin with $RCWV \leq 50\%$ and a peak in observation in the $70\% < RCWV \leq 80\%$ bin. It is worth noting the increasing trend in the number of observations per bin for the cases in the 330° to 70° sectors with wind speed $\geq 5\text{m/s}$ (circles in figure 15a), i.e. we are experiencing more days with high tropospheric moisture content in this sectors, particularly in the 20° to 70° sector. As shown in table 3.2, the sectors from 0° to 70° are exposed to the South China Sea and thus this observed trend in RCWV seems to support our conjecture on the advection of high moisture contents from the oceanic track.

Figures 16a and 16b show that the steady increasing trend in precipitation-CWV relationship is generally not affected by the wind conditions at 800hPa. They do show some impact on the rainfall intensity, particularly in the 330° to 70° sector (yellow, pale blue and black lines). Much heavier rainfall, a 'sharp pickup' in intensity from the $70\% < RCWV \leq 80\%$ bin to the $RCWV > 80\%$ bin, is being observed under the condition with the wind speed $> 5\text{m/s}$ over these sectors. There is good reason for us to trust this 'sharp pickup' in precipitation to be related to the increase in the moisture content; the sectors show an increase in the number of observations between these two bins and a 'sharp increase' in the precipitation rate. A departure from the steady increasing trend is being observed in the 0° to 20° sector in the wind speed $\leq 5\text{m/s}$ regime (pale blue line in figure 16a) contrast to the 'sharp pickup' in the wind speed $> 5\text{m/s}$ regime further indicate the advection of moisture is playing an important role in this sector.

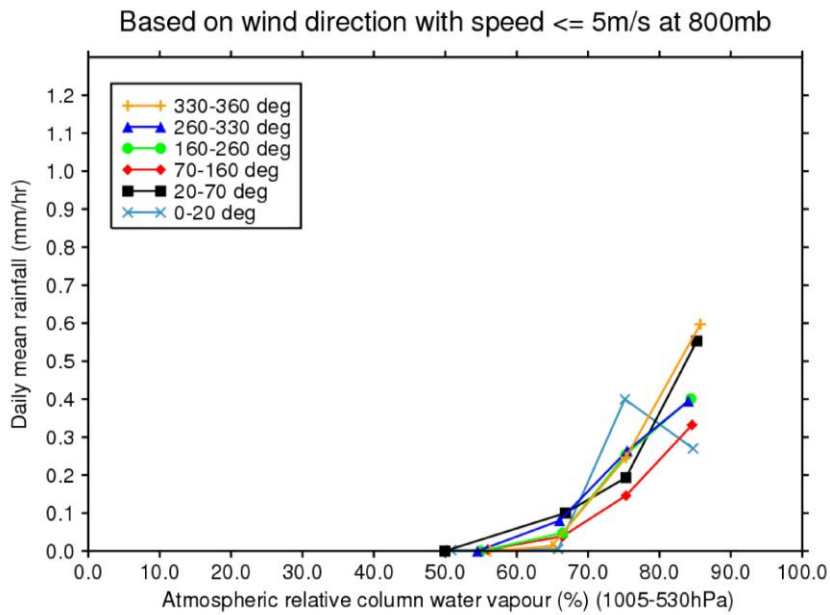


Figure 16a: Daily mean rainfall (mm/hr) conditioned on tropospheric relative column water vapour (%); wind speed $\leq 5\text{m/s}$ at 800 hPa.

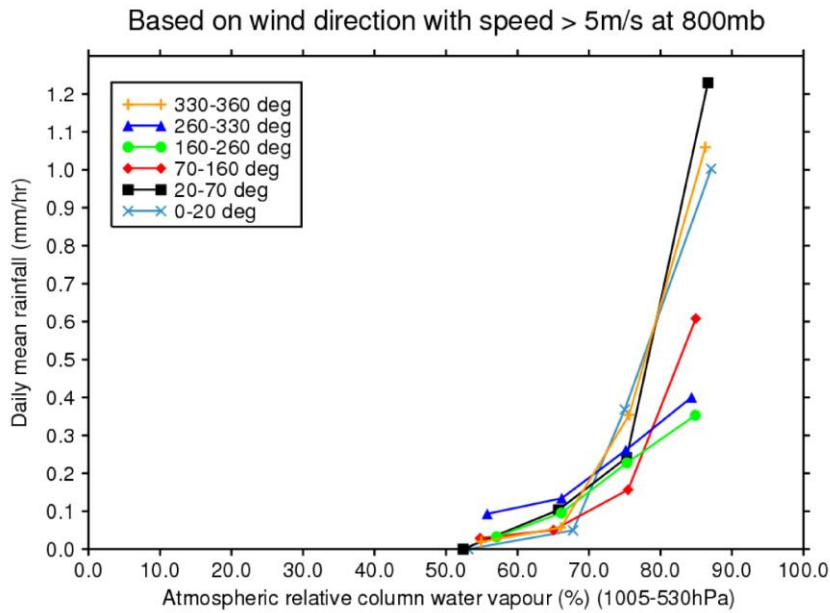


Figure 16b: Daily mean rainfall (mm/hr) conditioned on tropospheric relative column water vapour (%); wind speed $> 5\text{m/s}$ at 800 hPa.

3.6 Precipitation Lag-Lead analysis

A question which naturally follows from the preceding analysis is whether increased tropospheric moisture enhanced convection or whether the atmosphere moistens by the convective activities. Studies indicate feedbacks in both directions.

Sherwood and Wahrlich (1999) found that CWV was elevated within 3 hours of convective onset, with peak CWV occurring just after onset or during ongoing convection. Mapes et al. (2006) showed positive moisture anomalies between 700 and 800 hPa several hours before and near the time of maximum rainfall. Holloway and Neelin (2009) showed that within six hours centered around heavy precipitation the atmosphere has already been moistened to near-maximum levels. Zelinka and Hartmann (2009) concluded that moistening occurs at low levels prior to convection and the humidity increase at upper levels and associated decrease in clear-sky longwave emission persist for many hours after the convective event.

These studies indicate that high CWV is not just associated with heavy rainfall itself, but often precedes precipitation. Brown and Zhang 1997; Sherwood 1999 and Tompkins 2001b indicate that an increase in lower-tropospheric moisture could play a causal role in enhancing convection by allowing entraining plumes to maintain higher buoyancy.

A lag-lead analysis on precipitation versus RCWV will thus next be investigated through a number of case studies. The timing (onset time and duration) of the precipitation events is estimated based on radar images obtained from the Meteorological Services Division, National Environment Agency of Singapore. The rainfall intensity is based on the same daily mean rainfall obtained from the gauge in this study. It should be pointed out here that a much larger dataset would be required in verifying the robustness of the results to be presented.

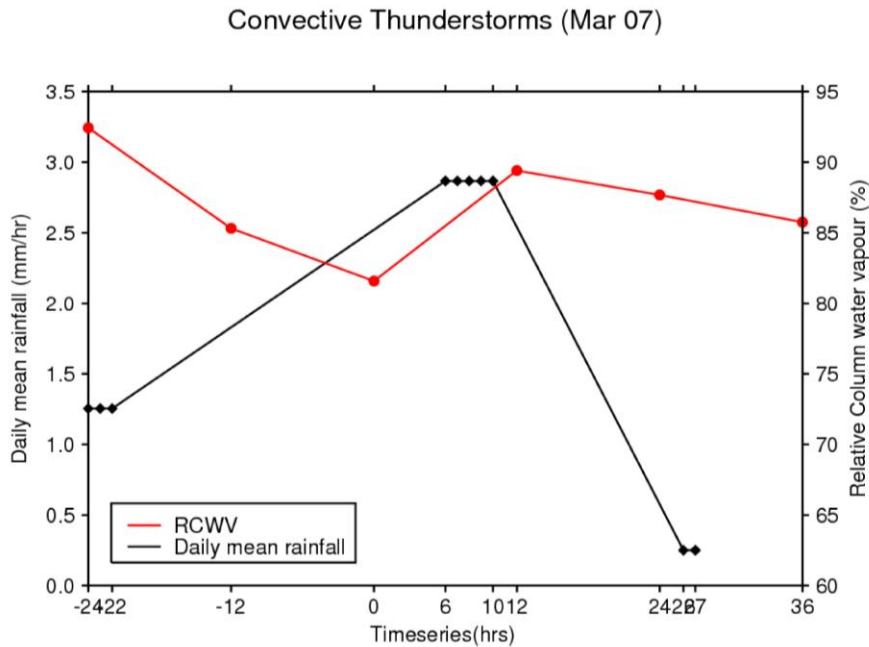


Figure 17: Time series of daily mean rainfall (mm/hr) and RCWV (%)

Figures 17 - 19 show the time-series of precipitation and RCWV for several events. Note that for figures 17 – 19, the 0 hrs and 12 hrs on the time-axis are the times where the 0000Z and the 1200Z sondes launched on the day of our focused precipitation event. -12hrs and -24hrs denote the 1200Z & 0000Z launches the previous day; 24hrs and 36hrs, the 0000Z & 1200Z launches the following day. The other values on the time-axis indicate the onset and the end of the precipitation event. (e.g. in figure 17, our chosen event starts around 0600Z and ended around 1000Z). Another point to note is that the hourly rainfall is taken as an average over the whole day rather than over the event duration and is plotted as a constant value for the whole precipitating duration.

Figure 17 shows a typical diurnal-dominated convective event with late afternoon thunderstorms (0600Z to 1000Z; local time 2-6pm). It can be seen here that there is no indication of an increase (indeed a decrease from previous day) in RCWV 6 hours before the onset of a precipitation event and the troposphere remains relatively moist 2 hours after precipitation.

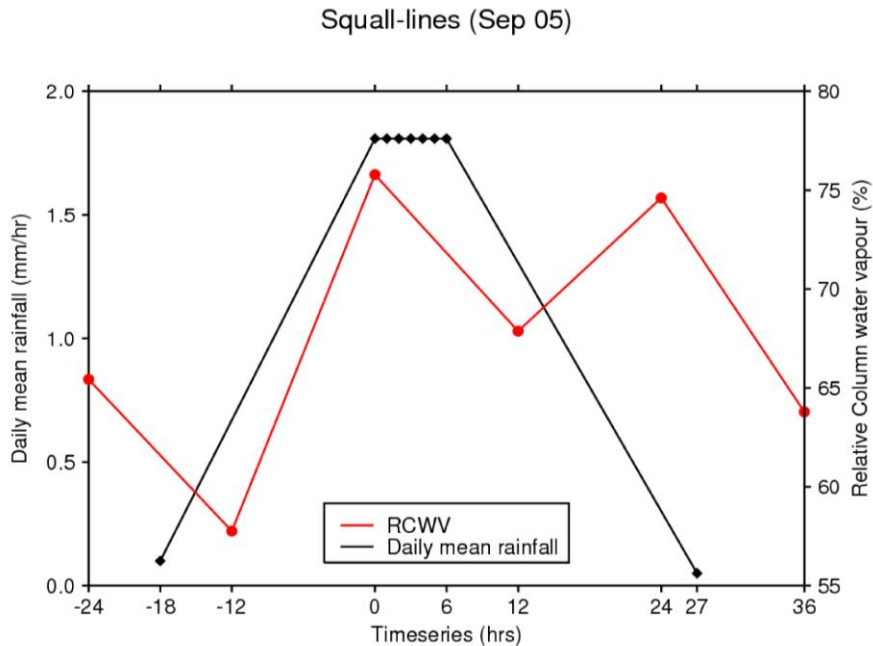


Figure 18: Time series of daily mean rainfall (mm/hr) and RCWV (%)

A typical early morning squall-line affecting Singapore is shown in figure 18. It is clear that the RCWV was elevated during the ongoing convection and we do observed a drop in RCWV 6 hours after the convective activity; there is a clear signature that higher moisture content is associated with the day affected by the squall-line. A pickup in RCWV was observed in the 0000Z (24hrs) data the following day, 3 hours ahead of some light precipitation. It would appear here that precipitation moistens the atmospheric column through moisture convergence and evaporation; this positive feedback will most likely enhance the possibility of the next precipitation event.

Figure 19 shows the relationship between the variables during a wet NE monsoon surge event. It is not a surprise to observe high RCWV along with the ongoing precipitation. Similar to the case in figure 18, a decrease in RCWV occurs 6 hours after the event. The following day's 1200Z sonde data do show an increase in RCWV from the 0000Z data 2 hours after the light precipitation on that day.

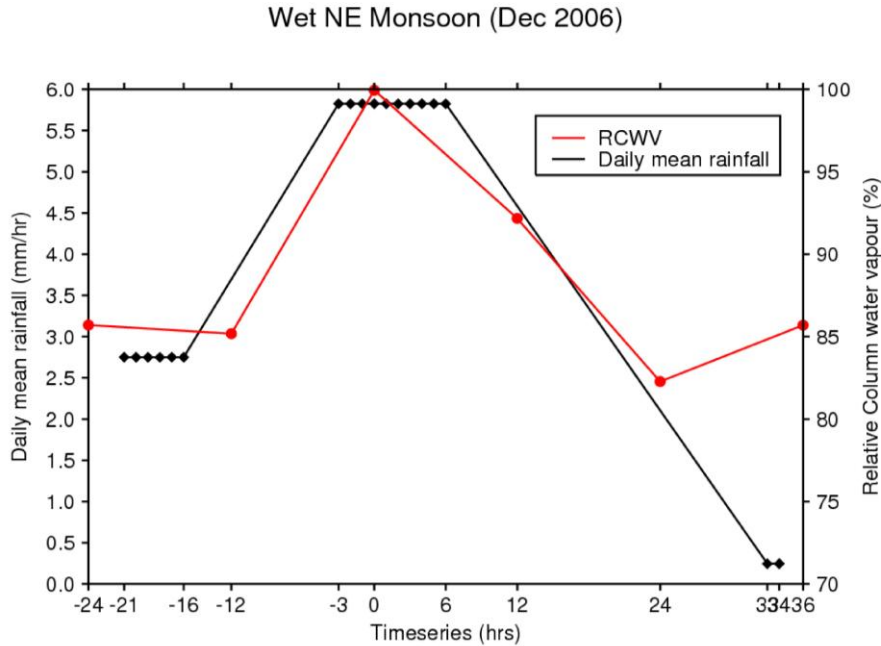


Figure 19: Time series of daily mean rainfall (mm/hr) and RCWV (%)

Another feature to be highlighted from these plots is that we do observe the diurnal cycle of the RCWV. A possible explanation for this is that without any influence from convective activity, the troposphere will be drier in the afternoon (associated with a larger dew point depression due to heating) and thus with a lower RCWV obtained from the 1200Z sonde. We thus retrieve relatively few observations in the higher ends of RCWV ($\geq 70\%$) and relatively more observations in the lower RCWV ($<70\%$) bins for the 1200Z sondes (Figure 1).

Three other case studies on intense locally developed convective thunderstorm, a long duration squall-line and a prolonged wet NE surge are presented in appendix B. Similar conclusion, i.e. high RCWV often precedes the rainfall by a few hours are shown there. This finding indicates that variation in RCWV could be considered as a precursor for the onset of precipitation.

We will next consider a possible explanation for the larger standard deviation in 1200Z RCWV relative to that in 0000Z, as highlighted in section 3.3. As discussed above, the atmosphere will remain moist several hours after precipitation. Locally developed

thunderstorms, with large variation in location and intensity usually occurs in the afternoon or early evening under the dominant influence of daytime boundary layer heating and ceases 1 to 2 hours before the launch of the 1200Z sonde. This indicates that the 1200Z RCWV is strongly influenced by the highly stochastic locally developed convective events relative to that retrieved in the 0000Z sondes and thus larger variation in RCWV evaluated at 1200Z will therefore be expected. RCWV evaluated at 0000Z will be influenced by well organized squall lines or large scale NE monsoons surge but a smaller deviation would be expected relative to that evaluated at 1200Z.

In summary, the results in this chapter have shown that although the steady increasing trend in precipitation with RCWV will be stronger during the wet NE monsoon, likely due to moisture and precipitation advection from the South China Sea, this steady increasing trend in precipitation-RCWV relationship holds in all seasons over Singapore. We thus conclude that the steady increasing trend in precipitation with RCWV is robust over both the tropical ocean (other studies) and tropical land (this study).

Chapter 4 Results II: Relationships between Column Water Vapour and Tropical Precipitation (Model simulations)

4.1 Introduction

As discussed in chapter 1, the ability to properly simulate deep convection and the corresponding cloud and humidity remains a challenge to GCMs. It was presented in chapter 3 that the action of tropical convection is sensitive to the free-tropospheric moisture content and thus in this part of the study, we aim to investigate how numerical models simulate the relationship between precipitation and CWV. The Unified Model simulated precipitation-RCWV relationship will be presented in section 4.2.

Model simulated moisture fields and their interaction with convection; particularly the contributing factors to the moisture variation will be carried out by analyzing the moisture budget over the simulated 30 day period and presented in section 4.3.

This project employs the UK Met Office Unified Model version 7.1 (UM). Impacts of the model resolution in simulating the precipitation-CWV relationship and the moisture budget will be examined by running the UM with grid length 40km ($0.375^\circ \times 0.375^\circ$) and 12 km ($0.11^\circ \times 0.11^\circ$). In general, we do expect a higher resolution model to perform better than its lower resolution counterpart due to an improved description of the impact of topography on atmospheric conditions and better representation of mesoscale details.

The model runs were done as part of the Cascade program. Cascade is a NERC funded consortium project to study organized convection in the tropical atmosphere using the Unified Model. Data from these runs are supplied by Dr Christopher E. Holloway who is working in this consortium project and co-supervisor of this study.

The model domain extends across the tropical Indian and western Pacific oceans for a thirty day period (starting from 0000Z 11 October 2008). A map of the entire and sub model domains selected in our study is shown in figure 20. Note that the initial data made available for the 40km run is 22S-21.554N 40E-179.446E and 22S-21.89N 40E-182.89E for the 12km run. The last eight grid points from each side of the initial entire

domain for the 40km run are trimmed so as to remove the boundary effects. The 12km run is then truncated to the same domain as the 40km run and thus a slight difference in boundary conditions will be expected for our runs. The entire domain used in our study is 19S-19N 42E-177E.

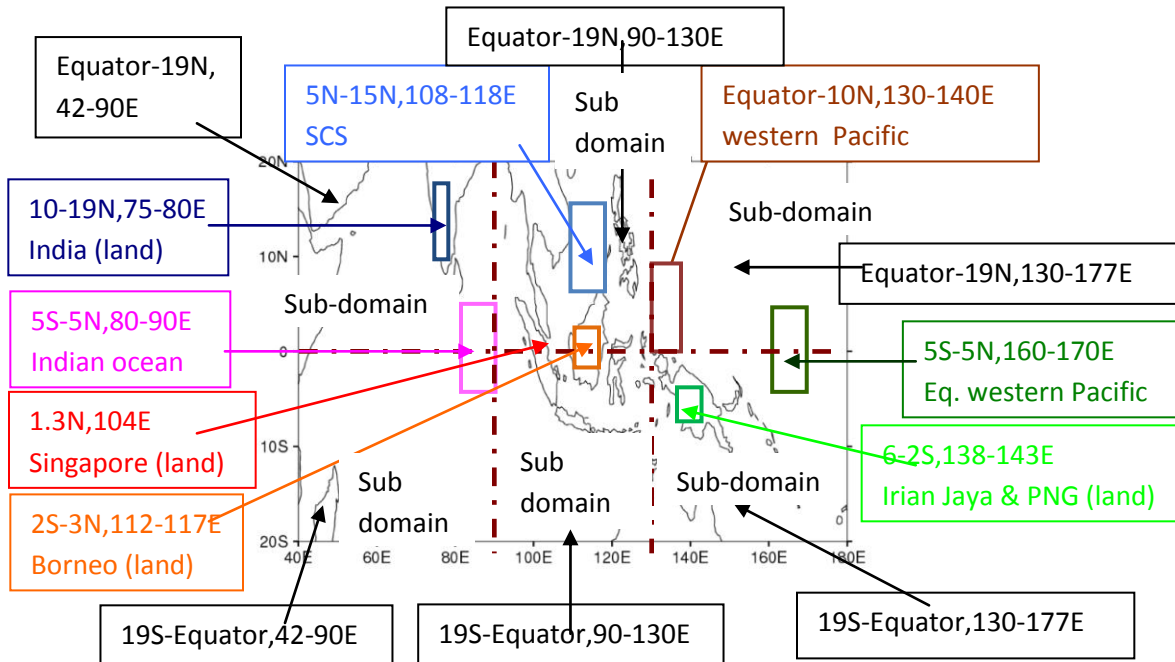


Figure 20: Entire model domain & Selected regions shown for the discussion

4.1.1 Model descriptions

Some technical information about the model (particularly, the UM convection scheme) taken from Met Office Unified Model User Guide (UM User Guide, 2004) is summarized here. The model runs on a rotated latitude-longitude horizontal grid with Arakawa C staggering and a terrain-following hybrid-height vertical coordinate with Charney-Philips staggering. The UM uses a mass flux convection scheme with convective available potential energy (CAPE) closure, this scheme is designed on the assumption that there are many clouds per grid-box and represents the transports of heat, moisture and momentum associated with cumulus convection within a model grid-box; it is used for

both precipitating and non-precipitating convection. The reader is referred to the Unified Model user guide (UM User Guide, 2004) for a detailed description.

4.1.2 Weather highlights over the thirty day period (11 Oct 2008 - 9 Nov 2008)

Our chosen domain was affected by three Tropical Storms over this simulated period.

On the 14 October, Tropical Storm 22W was formed in the in the northwestern South China Sea (near 18N 108E). Some of the South China island province and Vietnam were drenched by heavy downpours associated with this storm on 15-20 October 2008. Tropical Cyclone Rashmi was developed in the Bay of Bengal (near 17N 87E) on 26 October. Rashmi made landfall on 27 October in the south central coast of Bangladesh. Tropical Storm Maysak was formed on 7 November in the Philippine Sea (near 11N 115E) and tracked northward. (Source: Joint Typhoon Warning Center <http://metocph.nmci.navy.mil/jtwc.php>)

Although a formal validation will not be performed here, a subjective comparison between the simulated plots and satellite images suggests that model do simulate these storms reasonably well. These storms, however, will not have large impact on our results to be presented here as we will be examining our parameters through the averages over domains with much larger size relative to these storms' scale.

4.2 Relationship between precipitation and atmospheric moisture contents

It has been shown in Chapter 3 and other studies (Bretherton et al, 2004; Holloway and Neelin, 2009) that there is a positive correlation between precipitation and CWV in both the tropical land and ocean through observation analyses. This relationship study will be duplicated here through the model simulated data. Section 4.2.1 will present this precipitation-CWV relationship based on domain mean analysis. Results obtained through grid point analysis will be presented in section 4.2.2.

4.2.1 Precipitation and column water vapour relationship (Domain mean)

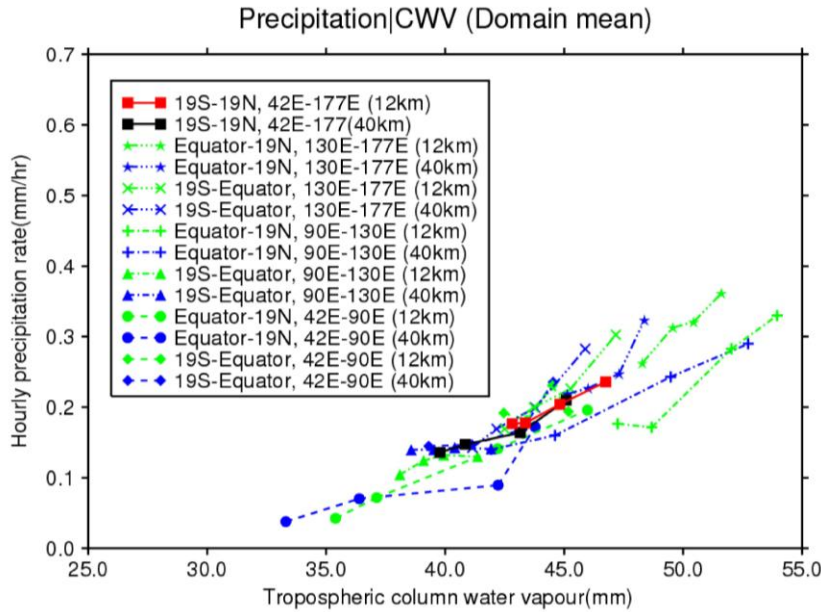


Figure 21: Domain mean hourly precipitation (mm/hr) conditioned on CWV (mm)
 Blue: 40km; green: 12km for respective sub-domains; black & red: 40km & 12km
 resolutions for the entire model

Domain mean quantities (i.e. the hourly averages of the model simulated parameters [CWV and precipitation] for all grid-points within the domain) will be considered in figures 21 and 22. The chosen model domain is divided into six sub-domains as indicated in figure 20. Data in the 40 km and 12 km runs are clustered into bins of 5mm and 3mm intervals in CWV within 30-55mm respectively. There is a total of 720 (30*24) data in each individual domain.

A positive correlation between the domains' mean hourly precipitation rate conditioned on CWV is shown in figure 21. The increasing trend in precipitation along with increasing CWV is exhibited in all sub domains. This positive relationship between the parameters is consistent with our observational analyses.

Figure 21 also suggests that the 12km run shows the pick-up in precipitation towards the higher end of CWV relative to the 40km run (the right shift). More discussion on this right shift in the relationship will be done in section 4.2.2.

Note that figure 21 is generated based on means taken over both the ocean and the land; this approach might mask the differences in simulating the precipitation-CWV relationship over the land and ocean. Below we further study the relationship between these parameters by further categorizing the model data into oceanic and land regions as defined in figure 20.

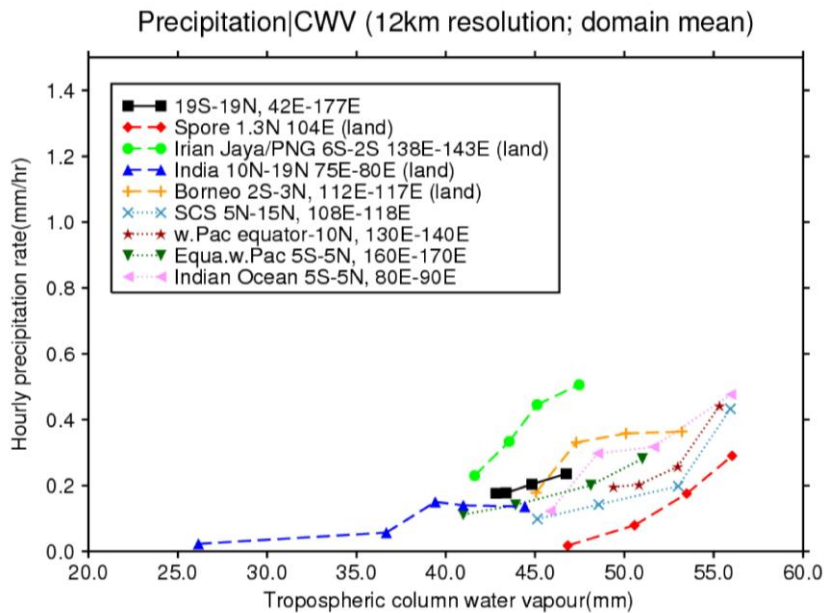


Figure 22: Domain mean hourly precipitation (mm/hr) conditioned on CWV (mm)
 Red, green, dark blue & orange dashed lines: Land; black: entire domain; last 4 dotted lines in the legend: Oceans. (12km run)

Figure 22 shows a stronger correlation (0.94 over the ocean vs 0.89 over the land) in the steady increasing trend of the precipitation with CWV over the ocean (dotted lines) than over the land (dashed lines). The steady increasing trend is not exhibited over Borneo and India (orange and dark blue dashed lines), particularly over their last two bins.

A most likely contributing factor to this departure from the general steady increasing in the precipitation-CWV relationship is due to the orographic effect which will be discussed further in section 4.3. We should, however, also note that there is a possibility that the model simulated relationship between precipitation and CWV is masked when

we consider the mean values over the domain. We should bare in mind the limited availability of the dataset (a total of 720 in each region) when considering these results.

4.2.2 Precipitation and column water vapour relationship (Grid points)

In view of the limitations of domain mean considerations, the relationship between precipitation and CWV will next be investigated based on the values at individual model grid points. This will provide us with more data points, 2,643,840 and 30,591,936 for the entire model domain in our 40km and 12km run respectively. Furthermore, the actual model simulated relationship between the parameters can also be examined.

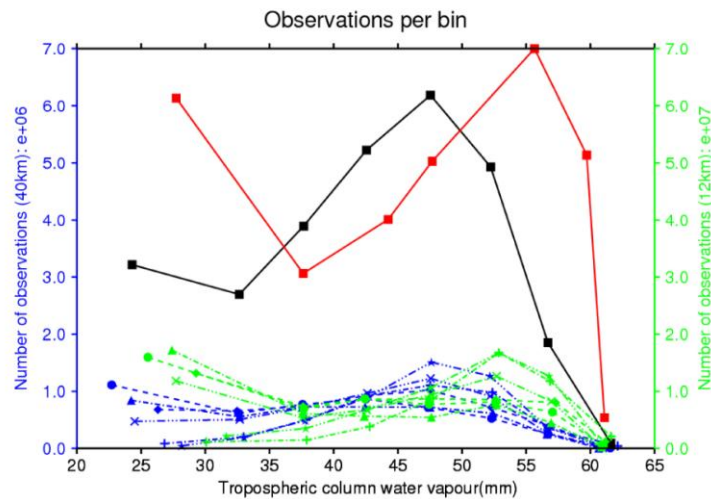


Figure 23: Number of observations in each bin. Blue: 40km; green: 12km run for respective sub-domains; black & red: 40km & 12km resolutions for the entire model. Left axis: 40km (of order 10^6), right axis: 12km (of order 10^7)
 'star': Equator-19N, 130E-177E; 'cross': 19S-Equator, 130E-177E;
 'plus': Equator-19N, 90E-130E; 'triangle': 19S-Equator, 90E-130E;
 'circle': Equator-19N, 42E-90E; 'diamond': 19S-Equator, 42E-90E

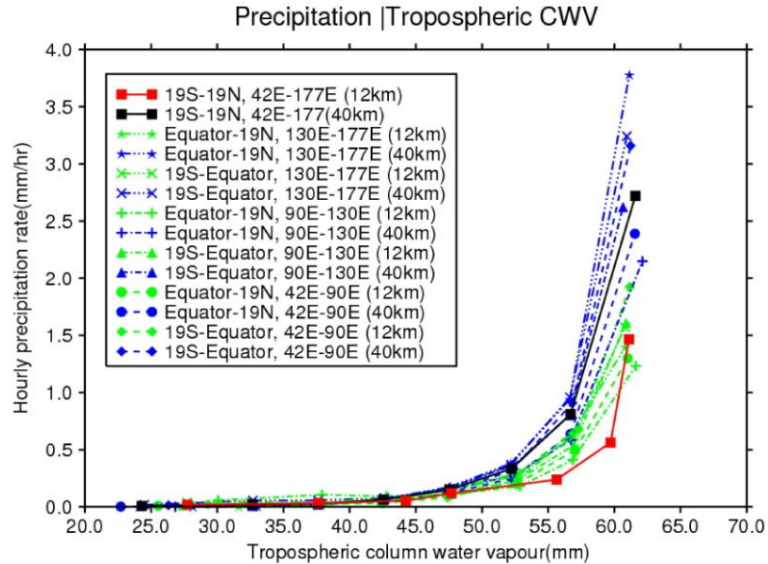


Figure 24: Hourly precipitation (mm/hr) conditioned on CWV (mm) Blue: 40km; green: 12km for respective sub-domains; black & red: 40km & 12km resolutions for the entire chosen domain.

Figure 23 shows the distribution of the data set clustered into bins based on CWV. The data are clustered into bins of 5mm intervals in CWV within 20-65mm. Note the difference in the order of magnitude on the Y-axes. Generally, the 40km dataset shows a peak in the 45-50mm CWV bin and the 12km dataset indicates a peak in the 50-55mm CWV bin; another point to note is that the 12km run do not have any data point with CWV < 25mm (the right shift mentioned in section 4.2.1). Both the dataset show the least number of data in the 60-65mm CWV bin (Much less for the 40km run).

It is clear from figure 24 that the model produces a very strong relationship between precipitation and CWV. A 'sharp pickup' in precipitation from the 55mm to the 60mm CWV bins is particularly simulated for the 40km runs (blue lines). The clear indication of heavier precipitation for the 40km runs relative to its 12km counterpart when conditioned on the same CWV bins is consistent with our finding based on the domain mean studies (figure 21). This observed difference in the simulated precipitation intensity for a given CWV is a model resolution effect. If the model were to simulate a similar amount of total precipitation in both the runs, we would be expecting that this total precipitation value to be shared by more data in the 12km run as shown in figure

23. For the empirical precipitation-CWV relationship to hold, the same CWV in 12km run will obviously correspond to a lower precipitation rate. For example, say we simulate a total precipitation of 300mm in a domain with 10 and 30 data points in the 40km and 12km runs respectively, with the same CWV throughout; we will have each data point in the 40km to simulate 30mm of precipitation while each data point in the 12km run to simulate 10mm of precipitation.

The steady increasing trend in precipitation with CWV simulated by both model runs in figure 24 is consistent with the analyses based on observations (chapter 3 of this report; Bretherton et al, 2004; Holloway and Neelin, 2009). We will proceed to investigate the similarities or differences in this relationship over land and ocean based on grid point data.

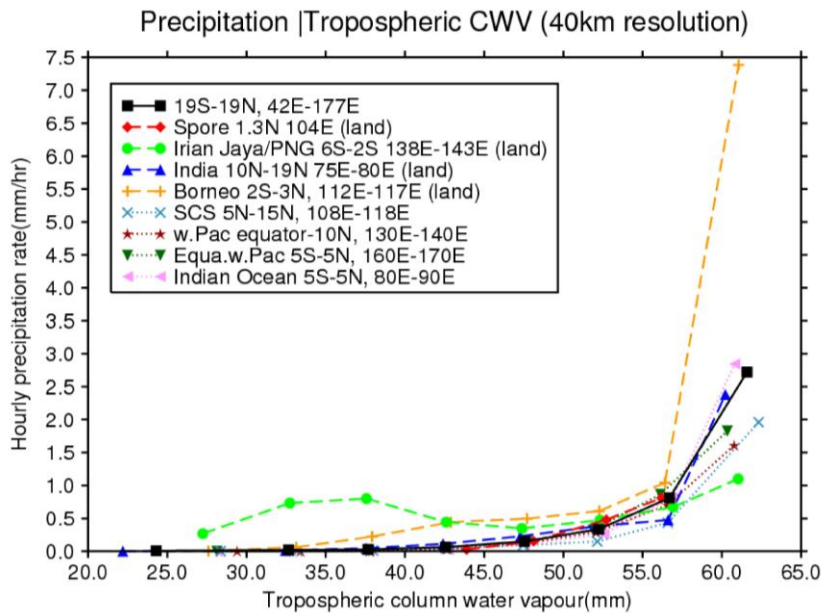


Figure 25: Hourly precipitation (mm/hr) conditioned on CWV (mm) Red, green, blue & orange dash lines: Lands; black entire domain; dotted lines: Oceans. (40km run)

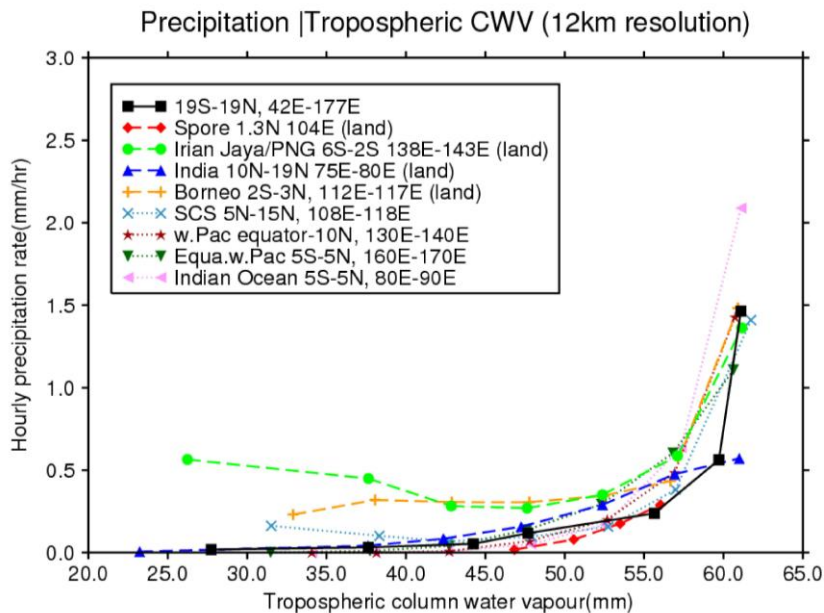


Figure 26: Same as figure 25 but for 12km run

Figures 25 and 26 compare the relationship between precipitation and CWV over land and ocean based on 40km and 12km model run respectively. The oceanic regions indicate a smooth increasing trend in precipitation with CWV for both model runs. This smooth increasing trend is however not clearly exhibited over the land, particularly over Irian Jaya and Papua New Guinea (light green circles). For example, there is a slight decreasing trend in precipitation from the 35mm to 40mm CWV bins over Irian Jaya and Papua New Guinea shown in both the 40km and 12km model runs. This departure from the steady increasing trend is most likely due to orographic effect in determining the precipitation-CWV relationship as stated in section 4.2.1. It is not surprise for us to obtain a higher precipitation rate in a lower CWV bin in regions comprise of both high elevated and lower terrains. While lower CWV corresponding to lower temperature will be expected over mountainous region; orographic lifting, on the other hand, will enhance the probability of heavier rainfall over this high elevated terrain. Relatively higher CWV will be expected in lower and thus warmer terrain. If the model were to simulate the same or even higher precipitation intensity over the high terrain region, higher precipitation rate with lower CWV as shown here will be expected. A precipitation-RCWV relationship would most probably lead to a steady increasing trend

over this high topographic region; however, no relevant data is available for us in justifying this hypothesis.

Another feature to note from figures 25 and 26 is that for a given CWV, the model is simulating more precipitation over the land than over the ocean, particularly over Borneo and Irian Jaya and Papua New Guinea, in the lower CWV bins. This observed relation is again speculated to be mainly due to the orographic effect in determining precipitation-CWV relationship.

The model, in general, does indicate a pickup in precipitation from the 55mm to the 60mm CWV bins in all regions for both the resolutions. We could generally conclude that the Unified Model does simulate the steady increasing trend in the precipitation with CWV reasonably well over both the tropical ocean and land.

4.3 Moisture budget

Having demonstrated on the ability for the Unified Model to simulate reasonably well the relationship between CWV and precipitation, we will now proceed to study how the model simulate the interaction between the precipitation, evaporation and column water vapour by analyzing the moisture budget. In particular, we will examine the contributing factors in the CWV variation. Sections 4.3.1 and 4.3.2 present the impacts on model resolution in simulating the budget terms. The contributing factors to the moisture variation on an hourly and daily time scales will be presented in sections 4.3.3 and 4.3.4 respectively.

4.3.1 Impact of model resolution (hourly precipitation, evaporation rates and Column Water Content)

Domain averages of the CWV, hourly evaporation and precipitation rates are shown in figures 27a and 27b for the 40 km and 12 km-resolution runs respectively. We observe a clear diurnal cycle in all the three parameters for both model runs. Both model runs show a drying trend and even dryer for the 40km run. The simulated CWV for the 12 km run is generally larger than that of its 40 km counterpart (consistent with figure 23). Particularly after 144 hours (6 days), the 40 km run shows a general decreasing trend

while the 12 km run persists with a relatively high CWV and indicates an obvious decreasing trend only after 288 hours (12 days). The difference in the intensity for this drying trend will be examined further in section 4.3.2.

The precipitation and evaporation trends, though of slight variation in intensity, do agree reasonably well with each other. These indicate that the relationship between CWV and precipitation are consistent for both model run but that the 40 km-resolution run has a higher precipitation rate relative to its 12 km counterpart corresponding to the same CWV which is consistent with our findings in section 4.2.1.

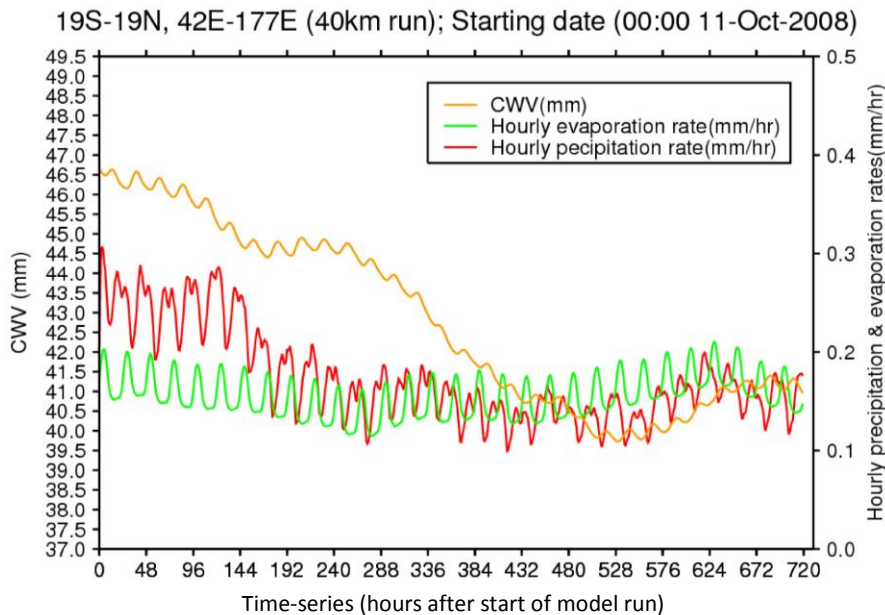


Figure 27a: Time series of CWV (mm), hourly precipitation and evaporation rate (mm/hr) [40km resolution run]

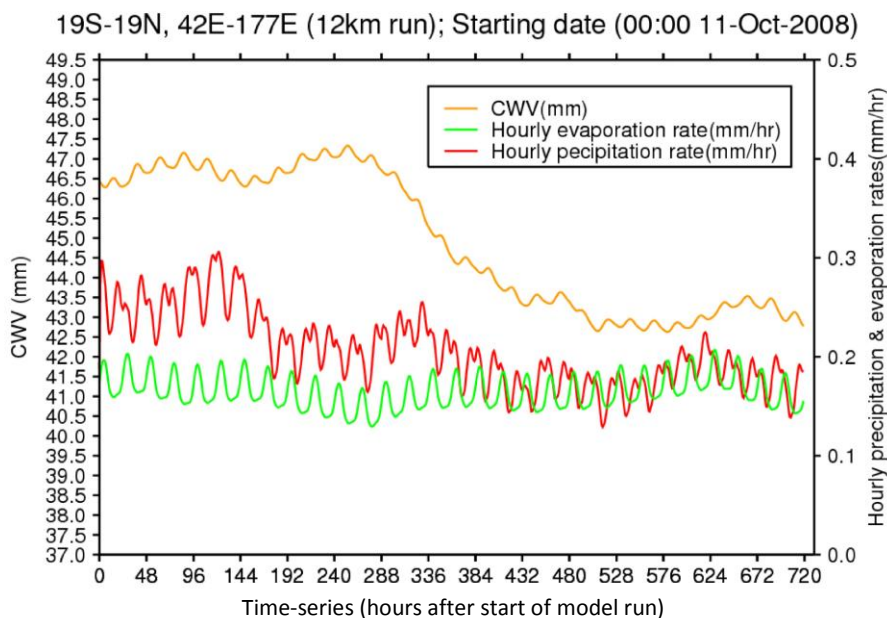


Figure 27b: Same as figure 27a but for 12 km resolution run

4.3.2 Impact of model resolution (Moisture budget: Hourly domain mean)

Moisture budget will next be analyzed through the numerical model simulated moisture fields and their interaction with precipitation.

Under the assumption that there are not big changes to the cloud water and ice in the atmosphere, we will consider our moisture budget through the following equation:

$$\text{Change in CWV} = \text{Evaporation} - \text{Precipitation} + \text{advection of CWV} \quad (4.1)$$

In practice, the advection of moisture will be taken as the residual of the evaporation, the precipitation and the change in vertically integrated column water vapour.

This assumption will be verified with the model simulated moisture advection.

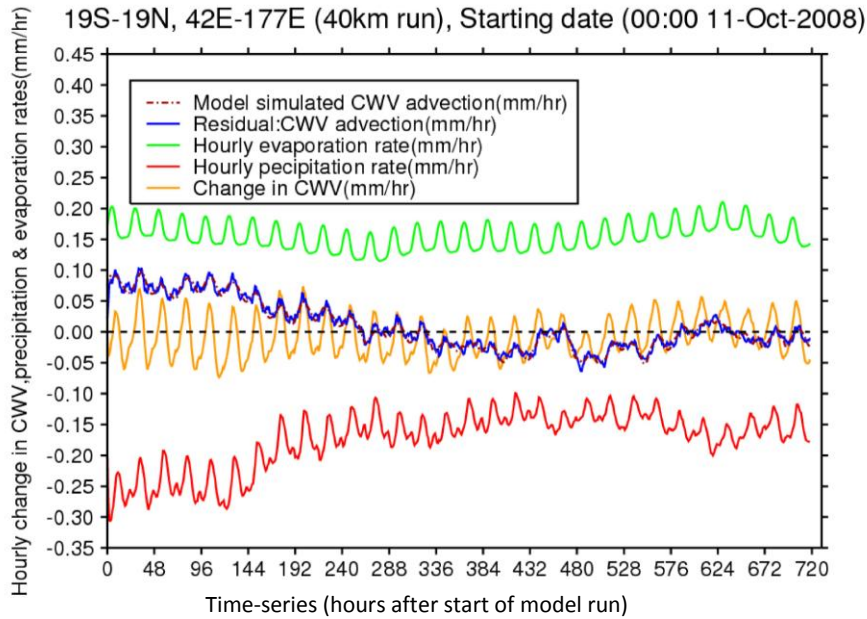


Figure 28a: Moisture budget based on equation 4.1 (40km run)
 Brown dot-lash line: model simulated CWV
 Blue line: residual; advection of moisture based on (4.1)
 Green line: hourly evaporation rate
 Red line: negative of the hourly precipitation rate.
 Orange line: change in CWV, taken to be the difference between the CWV over two consecutive hours

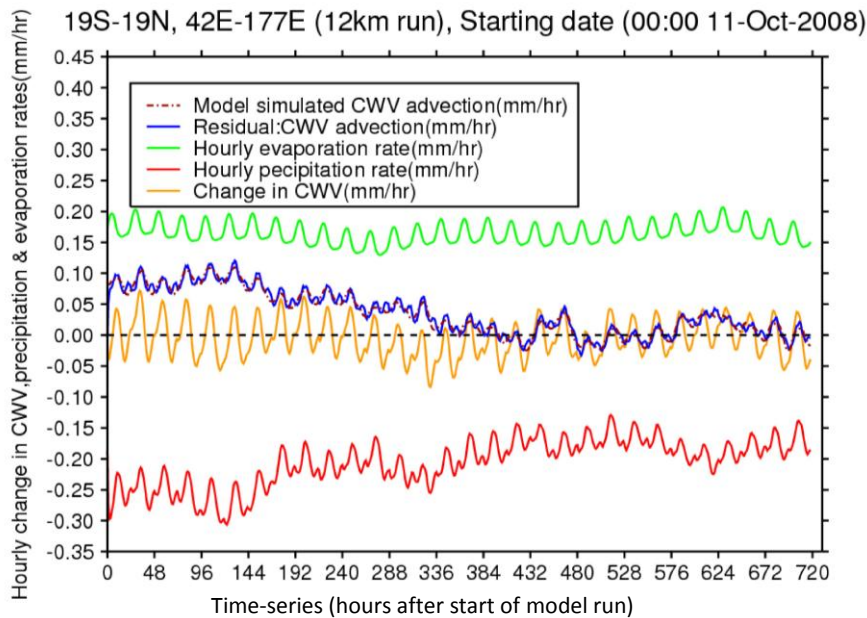


Figure 28b: Same as figure 28a but for 12km run

Figures 28a and 28b show that that our assumption in the formulating the moisture advection term based on equation 4.1 fits reasonably well with that from the model simulated CWV advection (blue solid line and brown dashed line). This increases our confidence in assessing the moisture fluctuations through equation 4.1.

Figures 28a and 28b also suggest that there is only slight variation in evaporation for both model runs but the 40km run seems to be constantly simulating a slightly lower evaporation rate at the lower end of the diurnal evaporation rate. The boundary conditions provide an import of moisture to the 40km and 12km runs over the first six and twelve days respectively. These advected moistures response with enhance precipitation and they contribute to a large part in the variation in CWV.

There is a negative correlation between the change in CWV and the hourly precipitation rate, i.e. decreasing trend in precipitation corresponds to an increasing trend in CWV. Moisture content is expected to be precipitated out during ongoing precipitation. This could also be interpreted as the accumulation of moisture precede and enhance the probability of relatively heavy precipitation or the further moistening of the atmosphere by the precipitation. It is worth noting here that Arakawa (2004) has pointed out that, although budget considerations are useful for many purposes, they can easily mislead our judgment of cause and effect. It should be interpreted as a feedback or adjustment rather than necessarily mean cause and effect.

As stated in section 4.3.1, the 40km run is simulating a dryer trend relative to its 12km counterpart; we will proceed to examine the role played by each term in contributing to the difference in this drying trend.

	40km run	12km run	Difference (40km-12km)
CWV advection (mm)	6.47272	26.1309	-19.6582
Precipitation (mm)	124.132	148.460	-24.3282
CWV advection – precipitation (mm)	-117.659	-122.329	4.66026
Evaporation (mm)	111.980	118.652	-6.67120
Change in CWV (mm)	-5.6511	-3.64779	-2.00330

Table 4.1: Budget terms in equation 4.1 over the 30 day period based on entire domain average

Table 4.1 compares the statistics of the budget terms for the two model runs over our 30 day period based on model domain mean. We observe from the Change in CWV that both model runs simulate a drying trend over the period with the 40km resolution run showing a relatively dryer trend than the 12km run. The difference in evaporation and CWV advection terms indicate even dryer for the 40km run but the total difference is reduced by the precipitation. The 40km run simulates a total of 26.3294mm (19.6582 + 6.67120) of moisture input into the atmosphere less than its 12km counterpart in this 30 day period but also with a total rainfall of 24.3282mm less. The relatively large difference in the CWV advection (19.6582mm) simulated suggests the important role played by the boundary condition in determining our model precipitation simulation.

We will next investigate further the robustness in the interaction between the moisture fields by subdividing our entire domain into six sub-domains (latitudes 42E-90E, 90E-130E and 130E-177E along with longitudes 19S-Equator and Equator-19N). The six sub-domains are shown on the domain map (figure 20).

Equator-19N, 90E-130E (12km run), Starting date (00:00 11-Oct-2008)

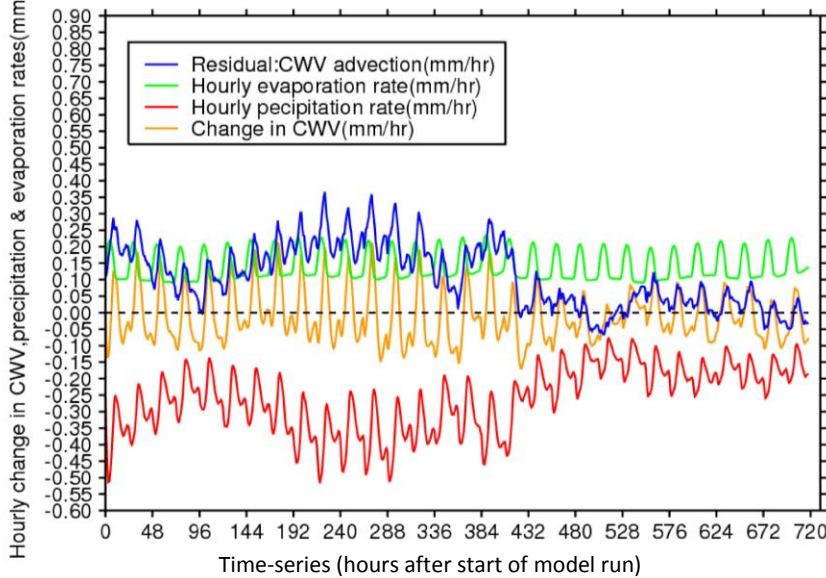


Figure 29a: Same as figure 28b but for domain Equator-19N, 90E-130E

Equator-19N, 130E-177E (12km run), Starting date (00:00 11-Oct-2008)

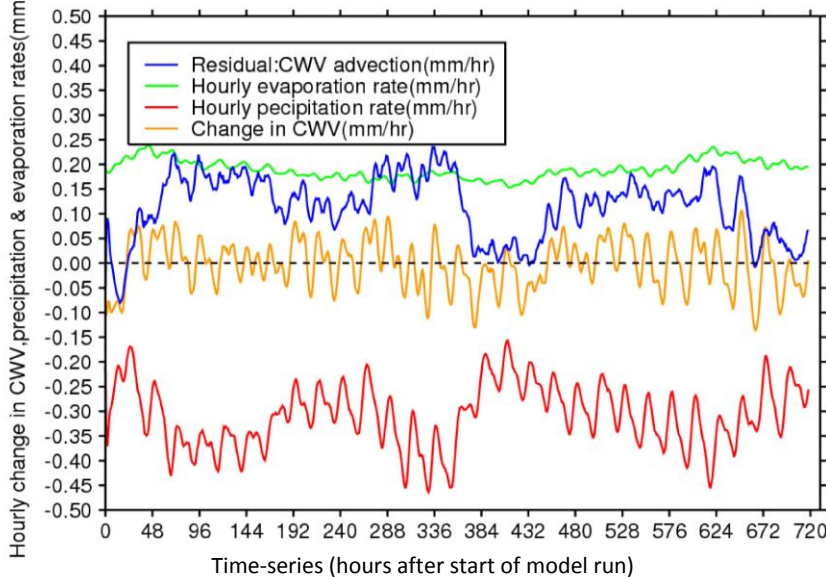


Figure 29b: Same as figure 28b but for domain Equator-19N, 130E-177E

Figures 29a and 29b show results for the sub-domains Equator-19N, 90E-130E and Equator-19N, 130E-177E respectively which we have chosen to present here to contrast the roles played by the budget terms over the land and ocean. Figure 29a consists of relatively large landmass: part of southern China, the SE Asia and the Philippines, while figure 29b consists mainly of the western Pacific Ocean.

Similar to figure 28b, the negative correlation between change in CWV and precipitation rate is again indicated here. There is a stronger diurnal cycle in all of the terms in figure 29a. A relatively lower evaporation rate is shown in figure 29a.

An interesting feature to highlight from figures 29a and 29b is the contribution of the evaporation rate (the green line) to the hourly change in CWV. Evaporation contributes to a large percentage of the diurnal CWV variation in figure 29a while moisture advection and precipitation are the major contributing factors to the CWV variation in figure 29b. There is a strong coupled between the precipitation and CWV advection (blue and red lines) shown in figure 29b over the western Pacific Ocean.

These interesting findings lead us to further investigate the contributing factors to the moisture variation between ocean and land.

4.3.3 Contributing factors to moisture content (Hourly domain mean: Land/Ocean)

Model domain is divided into land and ocean regions (see figure 20 for the regions). We present the 12km run for South China Sea and Irian Jaya and Papua New Guinea in figure 30a and 30b respectively. Figures 31a and 31b respectively show the moisture budget over Indian Ocean and Borneo for the 40km run. These figures are chosen to be presented here to indicate that the results to be discussed are site and resolution independence.

Figures 30a and 31a indicates there is little variation in the evaporation rate over the thirty day period for these oceanic regions. The moisture advection (the residual) and precipitation have large contributions to the moisture variation over the South China Sea and Indian Ocean. An obvious positive correlation between the moisture advection and precipitation suggests the dominating role played by the moisture advection in generating the precipitation over the ocean.

A relatively large diurnal cycle in all the parameters (the hourly precipitation and evaporation rates, the hourly change in CWV and the residual) is exhibited over the land (figures 30b and 31b). Evaporation contributes a relatively large portion of the variation in moisture content over these regions.

It is thus concluded, on an hourly basis, that moisture advection and precipitation play the major role in the CWV variation over the ocean while diurnal variation in evaporation, moisture advection and precipitation all contribute to a relatively large portion of the change in CWV over the land.

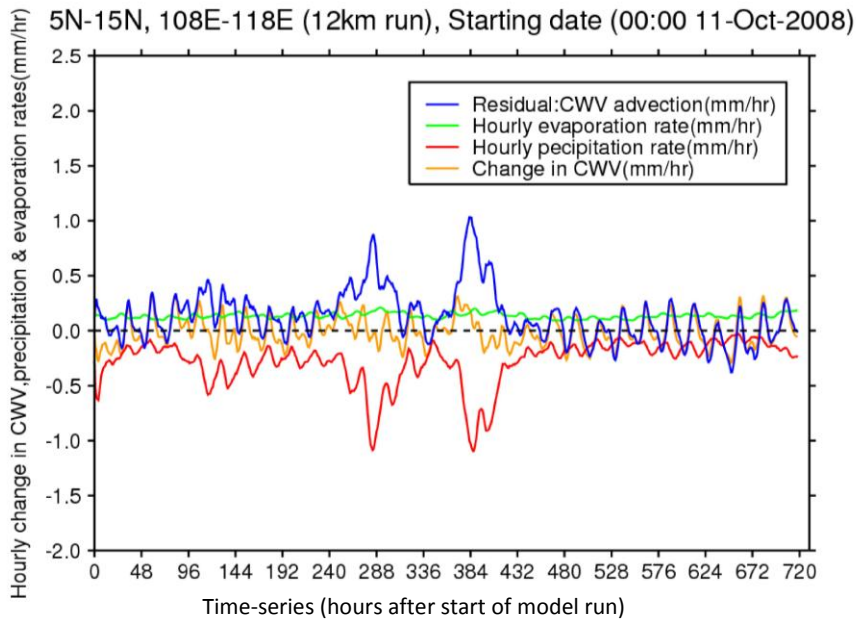


Figure 30a: Moisture budget based on equation (4.1); South China Sea (12km run)

Note that red line is the negative precipitation rate

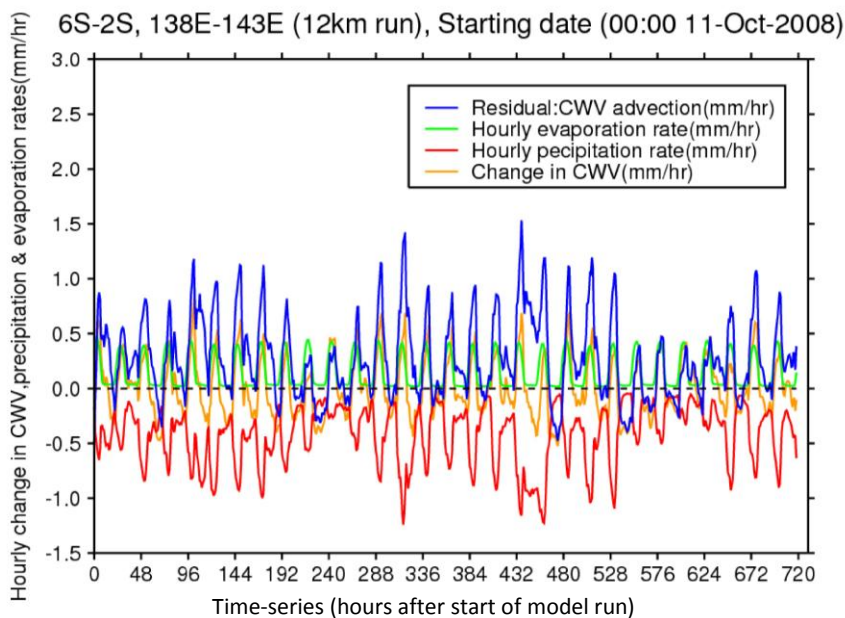


Figure 30b: Same as 30a but for Irian Jaya and Papua New Guinea (12km run)

Note that red line is the negative precipitation rate

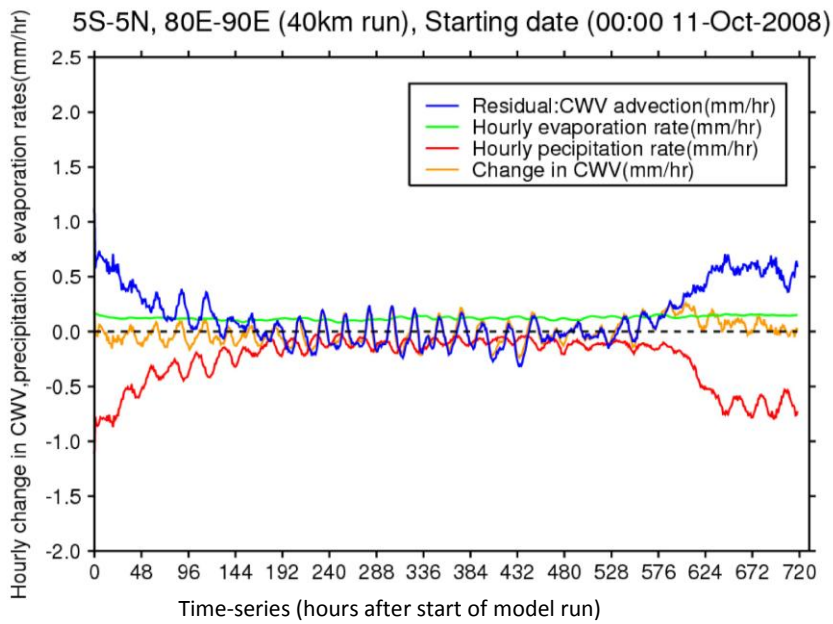


Figure 31a: Same as figure 30a but for Indian Ocean (40km run)
 Note that red line is the negative precipitation rate

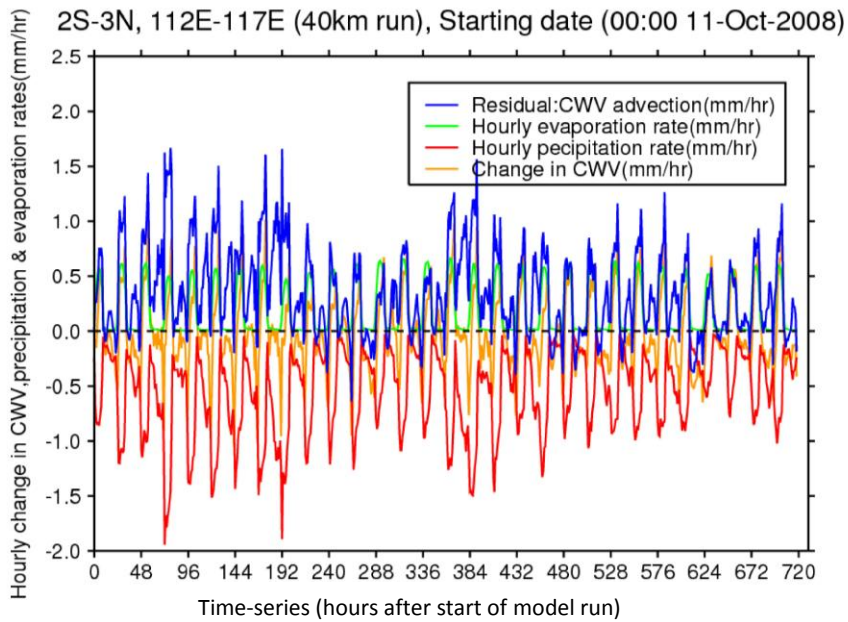


Figure 31b: Same as figure 30a but for Borneo (40km run)
 Note that red line is the negative precipitation rate

4.3.4 Moisture budget (Daily domain mean)

Having examined the moisture budget based on the hourly data in sections 4.3.2 and 4.3.3, we now approach this analysis on a daily time scale.

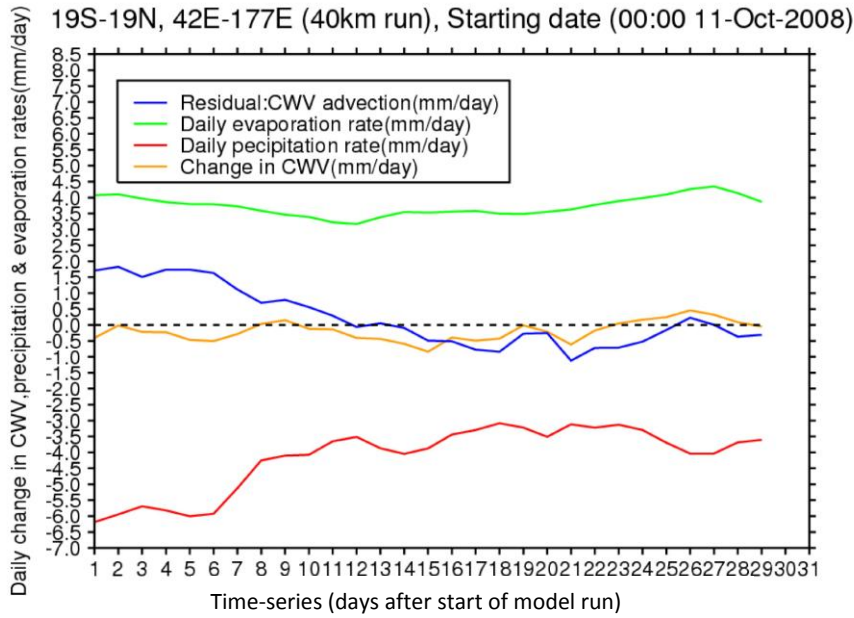


Figure 32a: Moisture budget based on equation 4.1; daily domain mean (40km run)
Note that red line is the negative precipitation rate

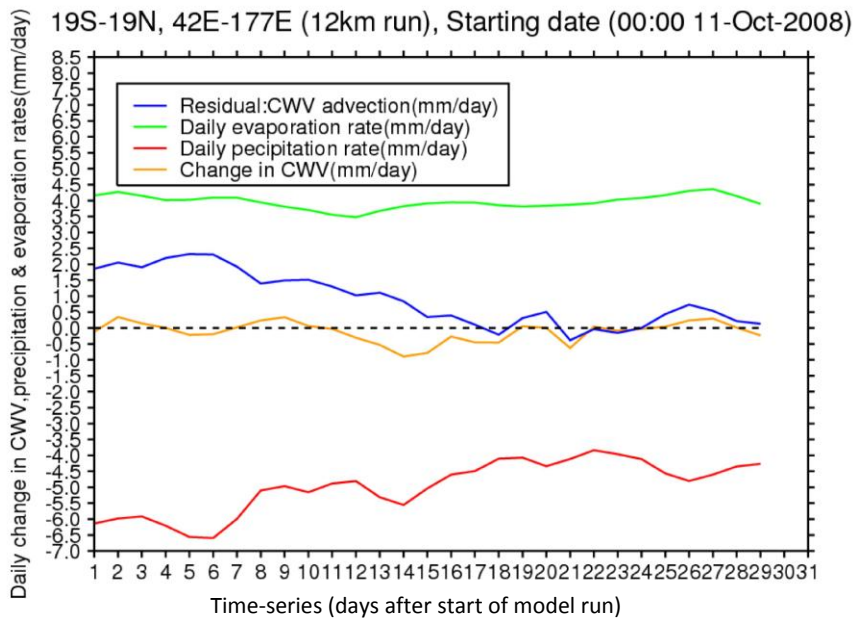


Figure 32b: Same as 32a but for 12km run
Note that red line is the negative precipitation rate

Figures 32a and 32b show the daily domain mean moisture budget (they may be compared with their hourly counterparts in figures 28a and 28b respectively). Both the runs indicate a relatively small variation in the evaporation rate over the simulated period. Figures 32a and 32b suggest generally the dominating contribution by moisture advection towards the variation in the precipitation (negative correlation between the blue and red lines: residual and negative precipitation rate respectively). This emphasizes the important role played by the moisture advection in simulating the precipitation rate.

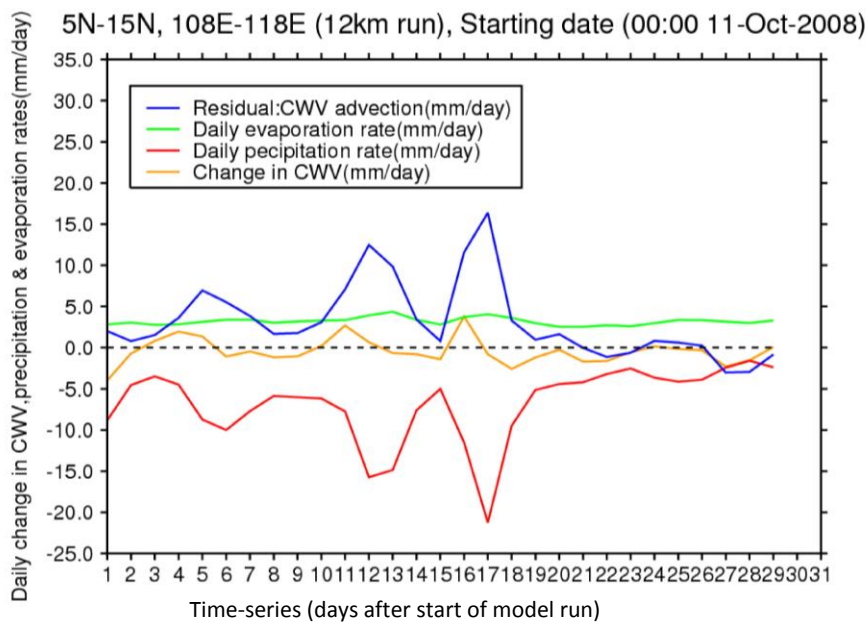


Figure 33a: Same as 32a but for South China Sea (12km run)

Note that red line is the negative precipitation rate

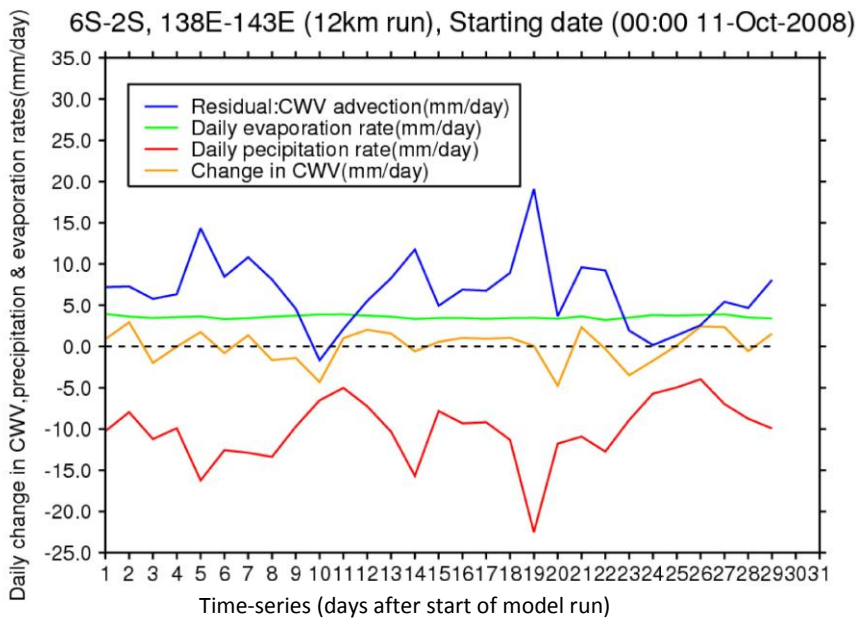


Figure 33b: Same as 32a but for Irian Jaya & Papua New Guinea (12km run)
 Note that red line is the negative precipitation rate

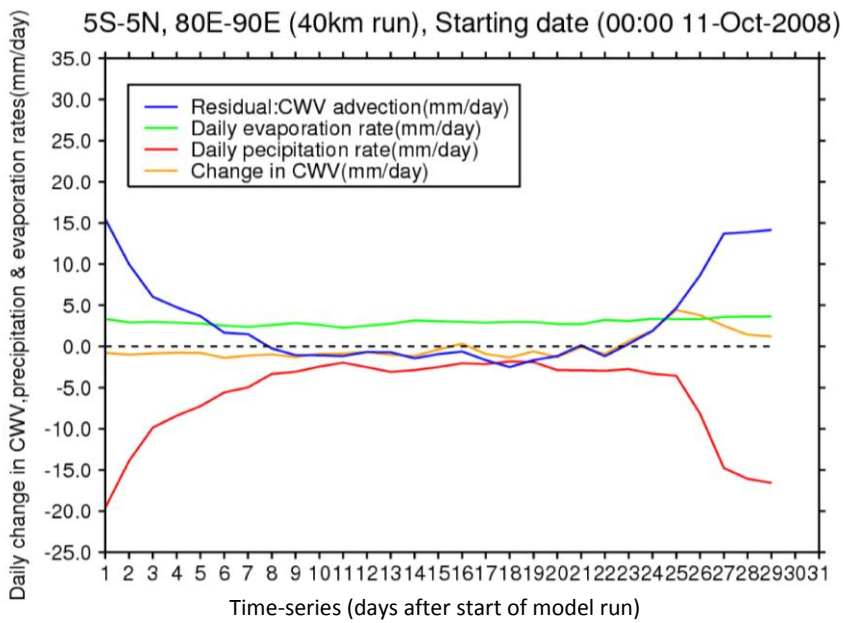


Figure 34a: Same as 32a but for Indian Ocean (40km run)
 Note that red line is the negative precipitation rate

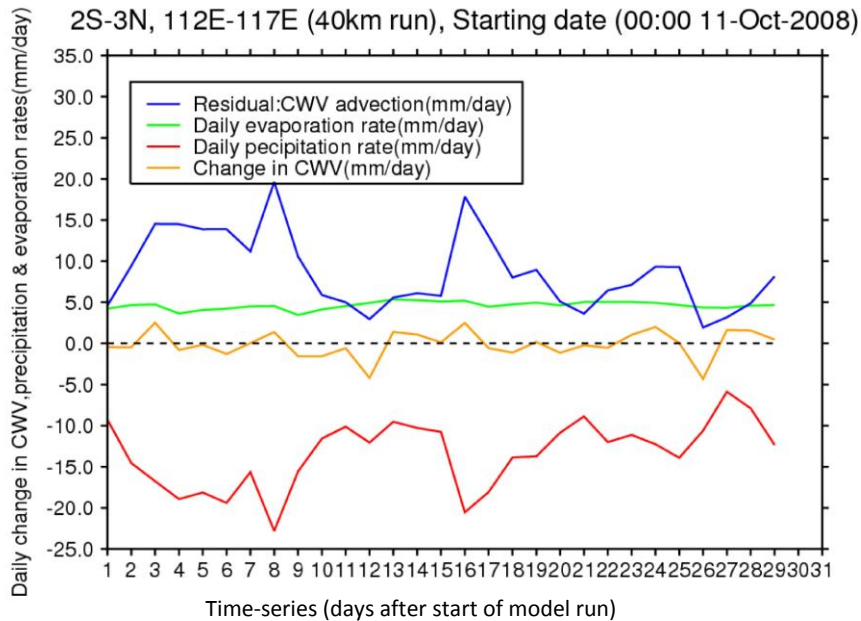


Figure 34b: Same as 32a but for Borneo (40km run)
 Note that red line is the negative precipitation rate

Figures 33-34 show the daily moisture budget over the South China Sea, Papua New Guinea, the Indian Ocean and Borneo respectively (figures 30-31 are their hourly counterparts). The relatively large contribution of the evaporation to the total variation in moisture content over land shown in section 4.3.3 through the hourly data is not duplicated here; moisture advection and precipitation are clearly the dominating factor in the moisture variation over both the ocean and land on a daily basis. There is a clear response of precipitation to the moisture advection on this daily time scale.

In summary, the Unified Model simulates the steady increasing trend in precipitation with CWV over both the tropical ocean and land reasonably well. The model also indicate that the diurnal cycle of the evaporation contribute to a relatively large portion on the variation of moisture content over the land on hourly basis. Moisture advection and precipitation are dominating the moisture variation over the land on a daily time scale. Over the ocean, moisture advection and precipitation clearly dominate the variation in the atmospheric moisture content in both time scales.

Chapter 5 Conclusions and summary

5.1 Summary of results

This report has focused on investigating the robustness in the steady increasing trend between precipitation and RCWV / CWV over the tropical Ocean and land. This was achieved using twelve years of precipitation gauge and radiosonde data from Singapore and 30 day period simulated data extending across the tropical Indian and western Pacific Oceans from the UK met office Unified Model (40km and 12 km runs).

5.1.1 Results from observation

In chapter 3, twelve years of precipitation gauge and radiosonde data from Singapore are used to examine the relationship between vertical structures of water vapour to tropical convection. There is little diurnal variation in the mean relative column water vapour (RCWV) and a large portion of the data lies between $60\% < \text{RCWV} \leq 100\%$ with a peak in the $70\% < \text{RCWV} \leq 80\%$ bins.

Moisture profiles conditionally averaged on precipitation show a strong association between rainfall and moisture variability in the lower free troposphere. Moisture above the boundary layer (850-550 hPa) is the key component in generating the steady increase in daily mean precipitation with RCWV. This finding reinforces the conclusions drawn from several studies (Sherwood 1999; Tompkins 2001; Bretherton et al. 2004; Holloway and Neelin 2009). This relationship holds for both the 0000Z and 1200Z dataset.

The median RCWV for all bins (except that of the $\geq 80\%$ bin in the wet NE monsoon) is zero indicate that the sufficiently high value (values vary between monsoons, ENSO episodes and diurnally) for relative column water vapour is a necessary but not sufficient condition for the development of intense precipitation. The daily mean rainfall used to derive such relationship coincides closely with the 75th percentile values for all bins. This indicates that we do observe more days with low precipitation in all bins and suggested the high possibility of the steady increasing trend in rainfall with RCWV to be

dominated by the relatively small number of extremely high precipitation events. It has also been illustrated that extremely high precipitations need not necessarily correspond to the highest RCWV.

The 'degree' of the pickup in precipitation with tropospheric moisture content is likely to be affected by large scale advection. Analytic results with data categorized based on 800 hPa wind conditions show that there is a high possibility that high atmospheric moisture content with high precipitation are being advected from the upstream oceanic regions, particularly during the wet NE monsoon seasons. Changes in tropospheric temperature are speculated not to be contributing towards the variation in the 'degree' of the steady pickup in the precipitation-RCWV relationship.

Lag-lead analyses on precipitation versus RCWV indicate positive moisture anomalies several hours before and after the precipitation events, consistent with the findings from Sherwood and Wahrlich 1999; Mapes et al. 2006; Holloway and Neelin 2009; Zelinka and Hartmann 2009.

In summary, although we do observe some variations in the 'degree' of relationship between precipitation and RCWV among seasons, the steady increasing trend in precipitation with RCWV is observed over Singapore. Due to the complexity of convective behaviour, this relationship might be site dependent and cannot necessarily be extended to other continental regions. Though the limited availability of dataset has to be taken into account in making the above conclusions, it nevertheless provides a useful result on the understanding of precipitation-RCWV relationship over tropical land.

5.1.2 Results from model simulation

In chapter 4, the reasonably well simulated steady increasing trend in precipitation with CWV over both the tropical ocean and land by Unified Model (UM) indicates that it does exhibit a reasonable sensitivity to the tropospheric moisture content.

The effect of topography on the precipitation-CWV relationship is presented. Lower CWV corresponding to cooler temperature over high elevated regions is expected; high elevated regions, on the other hand, tend to be affected by heavier precipitation. These generate the departure from the steady increasing trend in the relationship for regions consist of both high elevated and lower terrains in our study.

Moisture budget analysis indicates a drying trend over the simulated period. The 40km resolution run shows a relatively dryer trend than the 12km run. The highly coupled correlation between precipitation and CWV advection; together with relatively large difference in the CWV advection over evaporation simulated by both model runs; suggest the important role played by the boundary condition in determining our model simulated precipitation.

On an hourly timescale, diurnal variation in evaporation, CWV advection and precipitation all contribute to a relatively large portion in the variation of moisture content over land. CWV advection and precipitation play the major role in the moisture variation over the ocean on this hourly time scale.

Moisture advection and precipitation dominate the moisture variation for both the ocean and land on a daily timescale.

In summary, although there are some differences in the contributing factors to the simulated CWV variation and precipitation rates, the steady increasing trend between precipitation and CWV is reasonably well simulated by both the 40km and 12km Unified Model runs.

5.1.3 Conclusion

Summarizing all of these points, we do observe the steady increasing trend in precipitation rates with RCWV over both the tropical oceanic regions (previous studies) and tropical land (this study). The robust steady increasing trend in the precipitation-CWV relationship over both the tropical ocean and land is reasonably well simulated by the UK met office Unified Model.

5.2 Project Limitations

Main limitation to the work conducted in chapter 3 of this report was related to the small sample of data available which limits our in-depth study in the relationship between the atmospheric variables and rainfall intensity. It would be necessary to analyze a larger dataset for a robust conclusive relationship between the roles of moisture in controlling the tropical convection to be concluded. Furthermore, data from other tropical continents should be used in order to derive a data independent relationship. This could be achieved by the usage of remote sensing data in retrieving the atmospheric column water vapour for a wider spatial coverage. Higher frequencies of data would be required for a robust study in the precipitation lag-lead analyses; Zeng (1999) showed how supplementary use of satellite-derived column water vapour path could be used to improve predictions of tropical rainfall from infrared brightness temperature.

The unavailability of relevant data in computing RCWV in chapter 4 for our model simulation handicap us from verifying our hypothesis on the steady increasing trend in precipitation-RCWV relationship over high elevated regions (departure from the steady increasing trend in precipitation-CWV relationship).

5.3 Future works

In terms of extending the analysis conducted in this report there are further interest to expand on. The results presented in chapter 3 focused on just one location, Singapore. As stated in above, the results derived here cannot necessarily be extended to other locations due to the complexity of convective behaviour; it would be useful to repeat the study carried out in this report for other tropical land. One important result to verify is the robustness of the relationship in the steady increasing trend in precipitation with RCWV over tropical land, particularly in various monsoon seasons and ENSO episodes. It is argued here through a small number of case studies on the moistening of the atmosphere within several hours precede and after heavy precipitation, this argument obviously required further verification.

Concentration of atmospheric moisture is but one of the factors that can influence the development and intensity of precipitation. It would also be interesting to consider the influence of other atmospheric parameters in affecting the relationship between relative column water vapour and rainfall intensity, for example, through the multivariate approach, non-parametric methodology such as Neural Network, classification and regression trees model and clustering methods, etc...

The results presented in chapter 4 were reliant upon just one model (the Unified Model). To determine if these conclusions are general, or just limited to this model, it would be useful to repeat the study carried out in this report with other models.

The effect of model resolution in the precipitation-CWV relationship (the right shift for higher resolution model) indicated here should be verified with the Unified Model running with grid lengths of 4 and 1 km or even better, with other models.

The availability of relevant data in the near future would enable us to verify our hypothesis on the strictly increasing trend in precipitation-RCWV relationship over high elevated regions (departure from the steady increasing trend in precipitation-CWV relationship).

References:

- A. Arakawa 2004: Review Article, The cumulus parameterization problem: Past, Present and Future. *J. Climate*, **17**, 2493-2525.
- Betts, A.K., 1986: A new convective adjustment scheme. Part 1: Observational and theoretical basis. *Quart. J. Roy. Meteor. Soc.*, **112**, 677-691
- Betts, A.K., and C. Jakob, 2002: Evaluation of the diurnal cycle of precipitation, surface thermodynamics and surface fluxes in the ECMWF model using LBA data. *J. Geophys. Res.*, **107**, 8045-8057
- Bretherton, C. S., M. E. Peters, and L.E. Back, 2004: Relationships between water vapor path and precipitation over the tropical oceans. *J. Climate*, **17**, 1517-1528.
- Brown, R. G. and C. Zhang, 1997: Variability of mid-tropospheric moisture and its effect on cloud-top height distribution during TOGA COARE. *J. Atmos. Sci.*, **54**, 2760-2774.
- Colman, R.A., 2001: On the vertical extent of atmospheric feedbacks. *Clim. Dyn.*, **17**, 391-405
- Derbyshire, S. H., I. Beau, P. Bechtold, J.-Y. Grandpeix, J.-M. Piriou, J.-L. Redelsperger, and P. M. M. Soares, 2004: Sensitivity of moist convection to environmental humidity. *Quart. J. Roy. Meteor. Soc.*, **130**, 3055-3080.
- Holloway, C.E. and J.D. Neelin, 2009: Moisture vertical structure, column water vapor, and tropical deep convection. *J. Atmos. Sci.*, **66**, 1665-1683.
- http://app2.nea.gov.sg/topics_met.aspx, Meteorological Services Division, National Environment Agency of Singapore, accessed June 2009.
- <http://metocph.nmci.navy.mil/jtwc.php>, Joint Typhoon Warning Center, accessed August 2009.
- Lawrence, D.M., and P.J. Webster, 2002: The boreal summer intraseasonal oscillation: Relationship between northward and eastward movement of convection. *J. Atmos. Sci.*, **59**, 1593-1606.
- Lin, J.L. and coauthors, 2006: Tropical Intraseasonal Variability in 14 IPCC AR4 Climate Models. Part 1: Convective signals. *J. Climate.*, **21**, 5904 – 5924.
- Madden, R.A. and P.R. Julian, 1972a: Description of global-scale circulation cells in the tropics with a 40-50 day period. *J. Atmos. Sci.*, **29**, 1109 – 1123.

- Madden, R.A. and P.R. Julian, 1994: Observations of the 40-50 day tropical oscillation – a review. *Mon. Wea. Rev.*, **122**, 814-837.
- Mapes, B.E., and R.A. Houze, 1992: An integrated view of the 1987 Australian monsoon and its mesoscale convective systems. *Quart. J. Roy. Meteor. Soc.*, **118**, 927-963.
- McPhaden, M.J., 1999: Genesis and evolution of the 1997-98 El Nino. *Science*, **283**, 950-954.
- Moncrieff, M.W., 1992: Organized convective systems – Archetypal dynamic models, mass and momentum flux theory, and parameterization. *Quart. J. Roy. Meteor. Soc.*, **118**, 819-850.
- Neale, R. B., J. H. Richter, and M. Jochum, 2008: The impact of convection on ENSO: From a delayed oscillator to a series of events. *J. Climate*, **21**, 5904-5924
- Neelin, J. D., O. Peters and K. Hales, 2009: The transition to strong convection *J. Atmos. Sci.*, **66**, 2367-2384.
- Neggers, R., J. D. Neelin, and B. Stevens, 2007: Impact mechanisms of shallow cumulus convection on tropical climate dynamics. *J. Climate*, **20**, 2623-2642.
- Parsons, D. B., K. Yoneyama, and J.-L. Redelsperger, 2000: The evolution of the tropical western Pacific atmosphere-ocean system following the arrival of a dry intrusion. *Quart. J. Roy. Meteor. Soc.*, **126**, 517-548.
- Peters, O. and J. D. Neelin, 2006: Critical phenomena in atmospheric precipitation. *Nature Physics*, **2**, 393-396.
- Räisänen, J., 2007: How reliable are climate models? *Tellus*, **59**, 2-29.
- Redelsperger, J.L., D.B. Parsons, and F. Guichard, 2002: Recovery processes and factors limiting cloud top height following the arrival of dry intrusion observed during TOGA COARE. *J. Atmos. Sci.*, **59**, 2438 – 2459.
- Sherwood, S. C., 1999: Convective precursors and predictability in the tropical western Pacific. *Mon. Wea. Rev.*, **127**, 2977-2991.
- Sherwood, S. C., E. R. Kursinski, and W. G. Read, 2006: A distribution law for free tropospheric relative humidity. *J. Climate*, **19**, 6267-6277.

- Sherwood, S. C. and R. Wahrlich, 1999: Convective events and their environment. *Mon. Wea. Rev.*, **127**, 1777-1795.
- Shine, K.P. and A. Sinha, 1991: Sensitivity of the earth's climate to height-dependent changes in the water vapour mixing ratio. *Nature*, **354**, 382 -384.
- Slingo, J.M., K.R. Sperber, J.S. Boyle and J.P. Ceron, 1996: Intraseasonal oscillation in 15 atmospheric general circulation models: Results from an AMIP diagnostic subproject. *Climate Dynamics*, **12**, 325-357.
- Soden, B.J. and R.Fu, 1995: A satellite analysis of deep convection, upper-tropospheric humidity and the greenhouse effect. *J.Climate.*, **8**, 2333-2351.
- Spencer, R.W. and W.D. Braswell, 1996: How dry is the tropical free troposphere? Implications for global warming theory. *Bull. Amer. Meteor. Soc.*, **78**, 1097 -1106.
- Sun, Y., S. Solomon, A. Dai, and R.W. Portmann, 2006: How often does it rain? *J. Climate*, **19**, 916 – 934.
- Tompkins, A. M., 2001b: Organization of tropical convection in low vertical wind shears: The role of water vapor. *J. Atmos. Sci.*, **58**, 529-545.
- UM user guide, 2004: Unified Model User Guide, 2004
- Waliser, D.E., C. Jones, J.K. Schemm, and N.E. Craham, 1999: A statistical extended range tropical forecast model based on the slow evolution of the Madden-Julian Oscillation. *J. Climate*, **12**, 1918-1939.
- Yoneyama, K., 2003: Moisture variability over the tropical western Pacific ocean. *J. Meteor. Soc. Japan*, **81**, 317-337.
- Yang, Y.Y. and J. Slingo, 2001: The Diurnal Cycle in the Tropics. *Mon. Wea. Rev.*, **129**, 784-801.
- Zelinka, M.D. and D.L.Hartmann, 2009: Response of Humidity and Clouds to Tropical deep convection. *J. Climate*, in press. doi: 10.1175/2008JCL12452.1
- Zeng, X., 1999: The relationship among precipitation, cloud-top-temperature, and precipitable water over the Tropics. *J. Climate*, **12**, 2503-2514

Appendix A

Precipitation-RCWV relationship (ENSO within Monsoon seasons)

The results to be presented here follow from section 3.2.1 by further classifying the data within the Monsoons into ENSO episodes (figures A1, A2 and A3), the steady increasing trend in precipitation above a threshold RCWV still holds in general. However, we see that the relationship is no longer valid for some of the ENSO episodes considered in some Monsoon periods, for example, the La Nina condition in Wet NE and SW Monsoons shown in figure A1 and figure A2 exhibit a decrease in precipitation intensity from the $70\% < RCWV \leq 80\%$ to the $RCWV \geq 80\%$ bins (pale blue lines). Negative correlation between the variables was displayed in the El Nino episode during the inter-monsoon months (October and November) from the $70\% < RCWV \leq 80\%$ to the $RCWV \geq 80\%$ bins as well (Figure A3, red line).

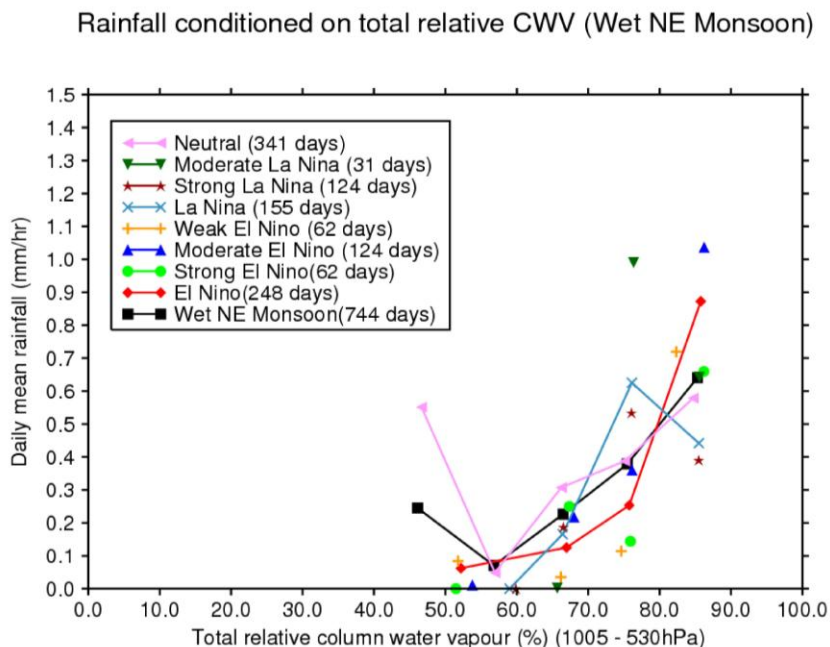


Figure A1: Average hourly precipitation rate (mm/hr) conditioned on tropospheric relative column water vapour (%), ENSO episodes within NE Monsoon.

Rainfall conditioned on total relative CWV (SW Monsoon)

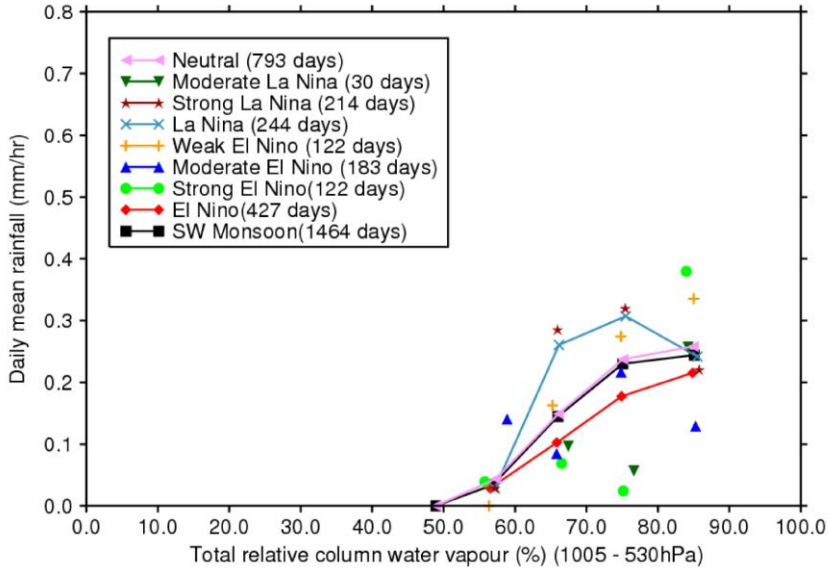


Figure A2: Same as figure A1 but with ENSO episodes within SW Monsoon.

Rainfall conditioned on total relative CWV (Oct, Nov)

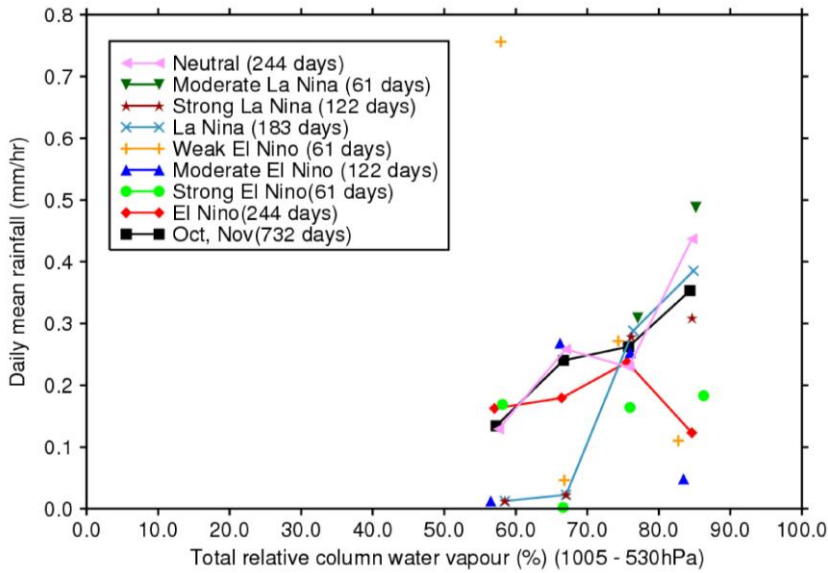


Figure A3: Same as figure A1 but with ENSO episodes within the inter-monsoon (October & November)

These departures from the usual steady increment relationship are most likely to be attributed to the limited number of observations available in representing the highly stochastic precipitation rates. Other plausible explanations for these departures might be the inhibition of precipitation in high RCWV conditions due to other atmospheric factors such as

- a) A very strong low-level vertical wind shear environment which inhibits the vertical development of convective clouds or
- b) The subsidence region within the vicinity of some convective activities which generate large relative column water vapour over the region.

These hypotheses, however, could not be investigated further due to a lack of availability of complementary observations.

Note that the discussions in this appendix are not meant to be conclusive with the limited dataset but aim at suggesting a possible starting point in data categorization for future studies.

Appendix B Precipitation Lag-Lead analysis (more case studies)

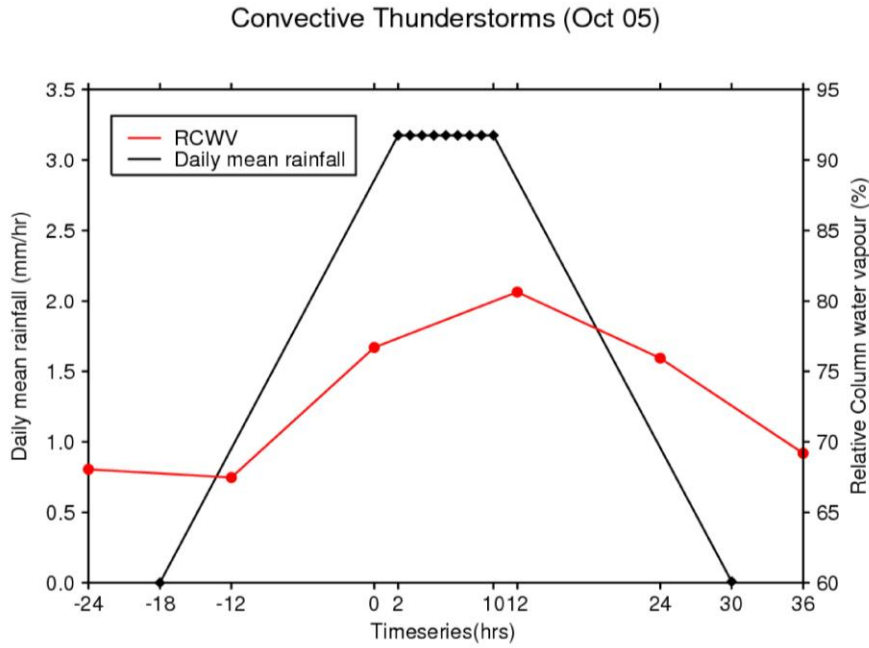


Figure B1: Time series of daily mean rainfall (mm/hr) and RCWW (%)

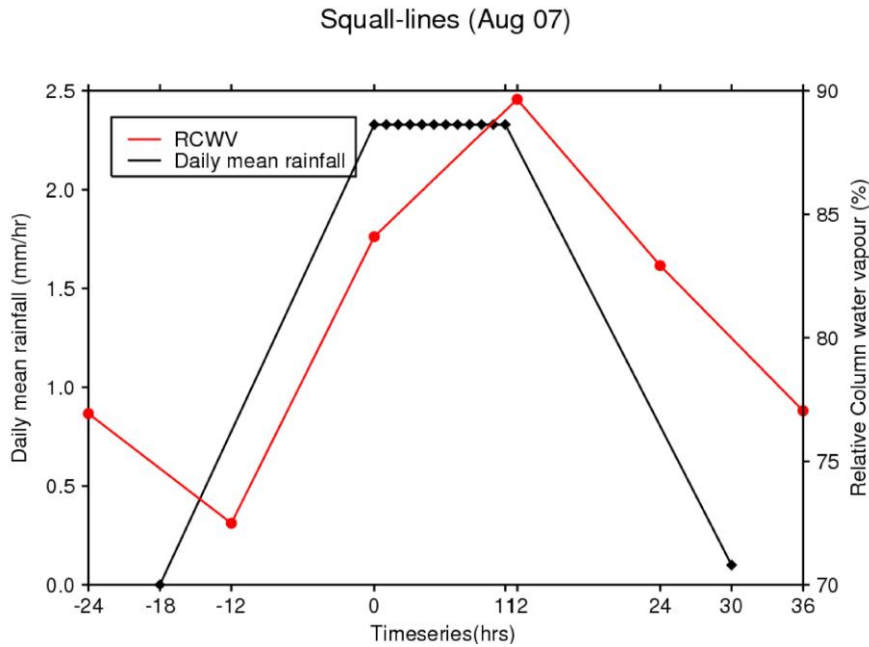


Figure B2: Time series of daily mean rainfall (mm/hr) and RCWW (%)

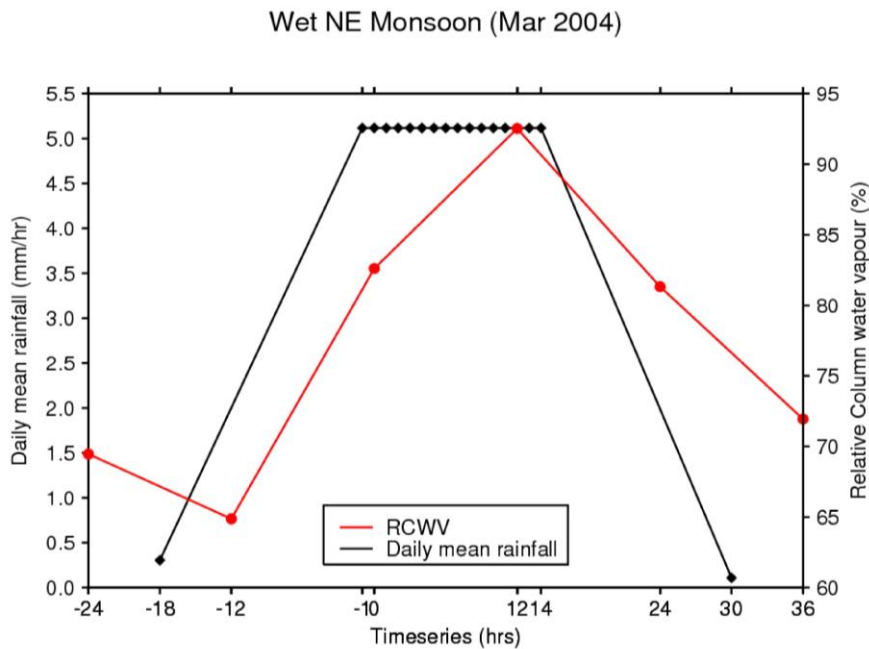


Figure B3: Time series of daily mean rainfall (mm/hr) and RCWV (%)

The results to be presented here further support the discussion in section 3.6.

Figures B1 – B3 present an intense locally developed convective thunderstorm, a long duration squall-line and a wet NE monsoon surge event respectively. All these long lasting precipitation events fall within 2 hours of the sondes' observation times and the increase in RCWV several hours before and after precipitation or along ongoing precipitation are indicated. These results are consistent with those discussed in section 3.6; i.e. high RCWV is not just associated with or after heavy rainfall, but often precedes the rainfall by a few hours. This finding further support our conclusion in section 3.6 that variation in relative column water vapour could be considered as a precursor for the onset of precipitation.

Appendix C Reference figures from other studies

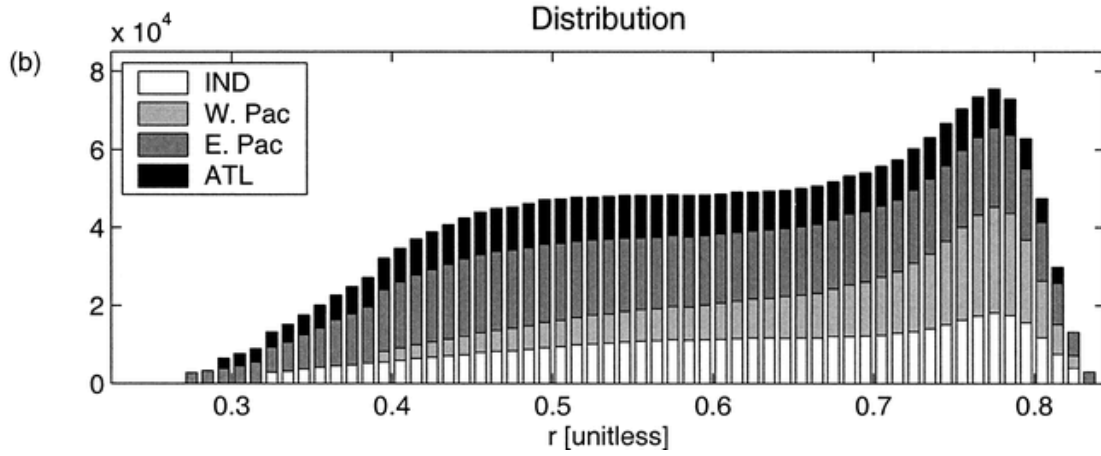


Figure C1 (Fig 3b in Bretherton et al., 2004): Number of observations in each bin in the four tropical ocean regions in their study.

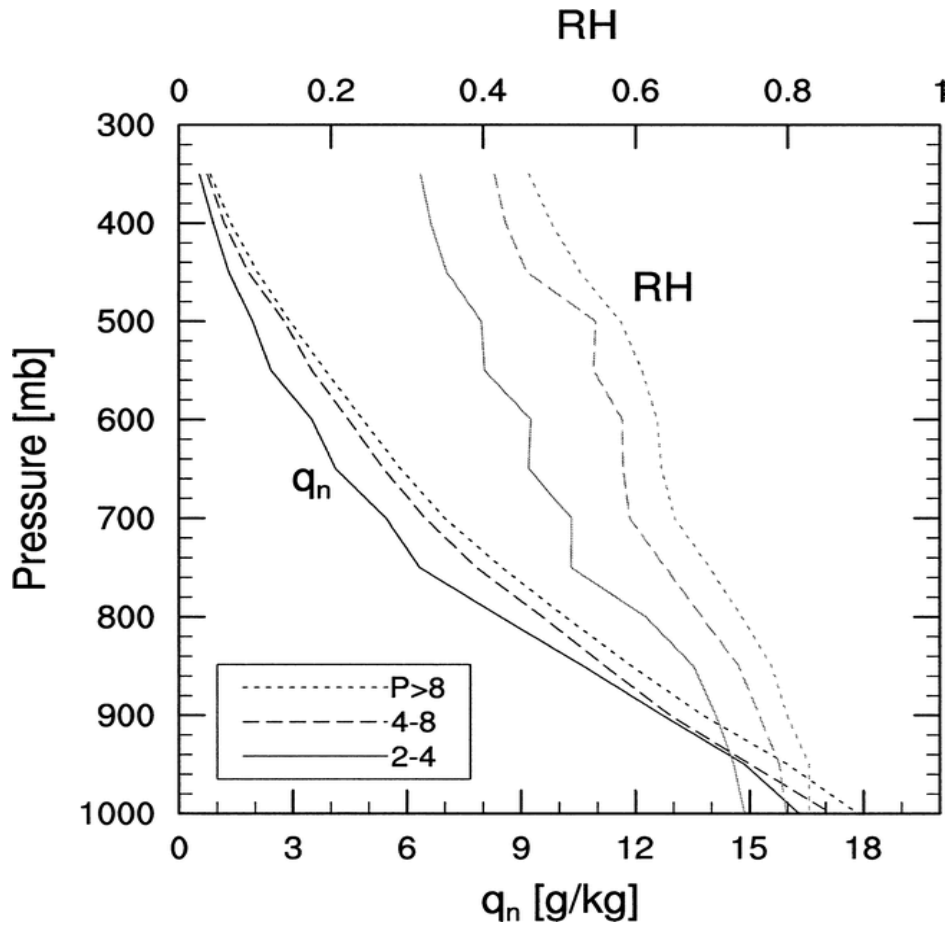


Figure C2 (Fig 9 in Bretherton et al., 2004): Radiosonde-derived profiles of normalized monthly mean specific humidity and relative humidity.

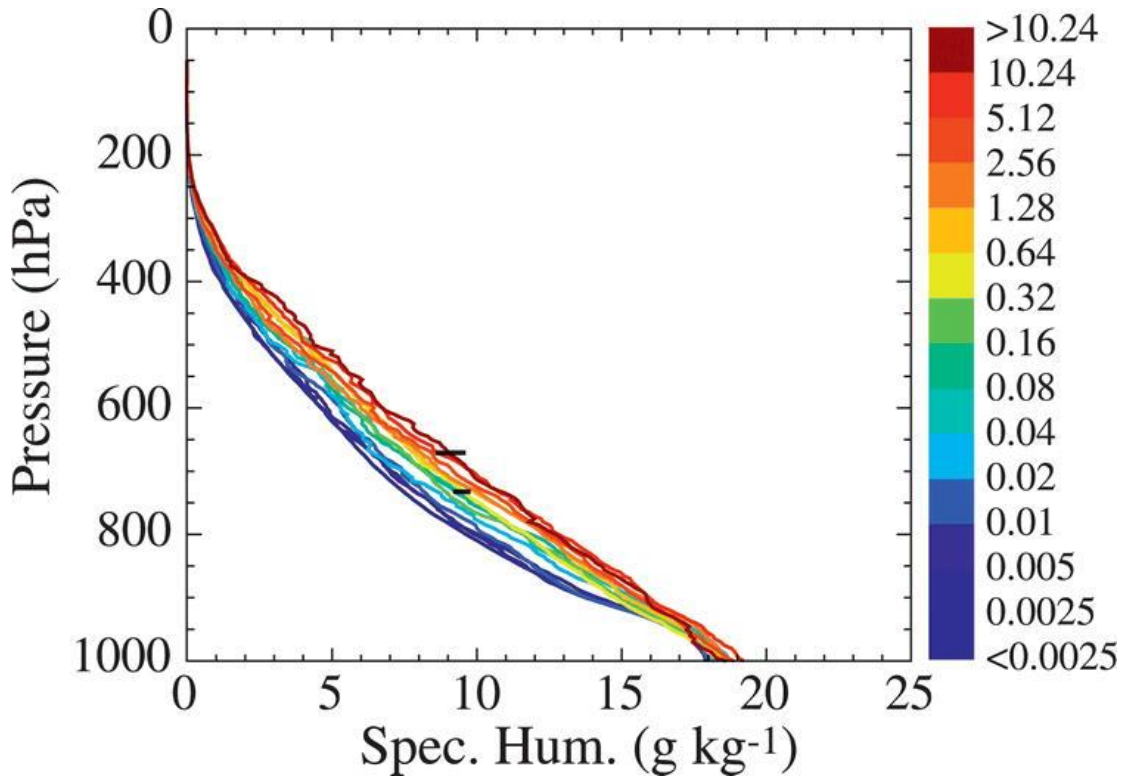


Figure C3 (Fig 1 in Holloway and Neelin, 2009): Specific humidity (g/kg) profiles conditionally averaged on 1-hr average precipitation rate in mm/hr.

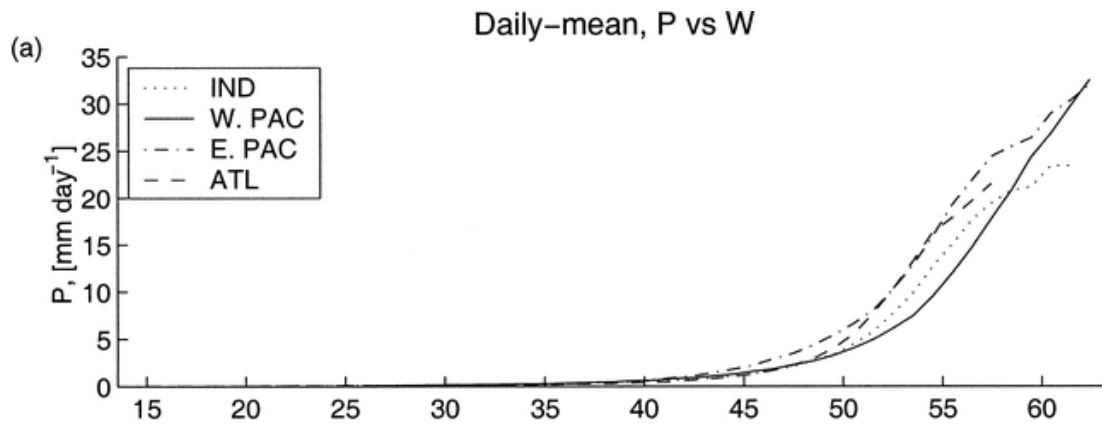


Figure C4 (Fig 2a in Bretherton et al., 2004): Mean daily averaged precipitation in 1-mm-wide bins of water vapour path for the four tropical ocean regions in their study.

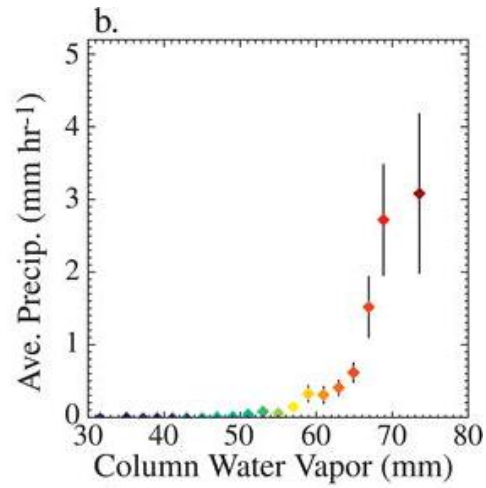


Figure C5 (Fig 3b in Holloway and Neelin, 2009): Precipitation rate (mm/hr) conditionally average on CWV in mm.

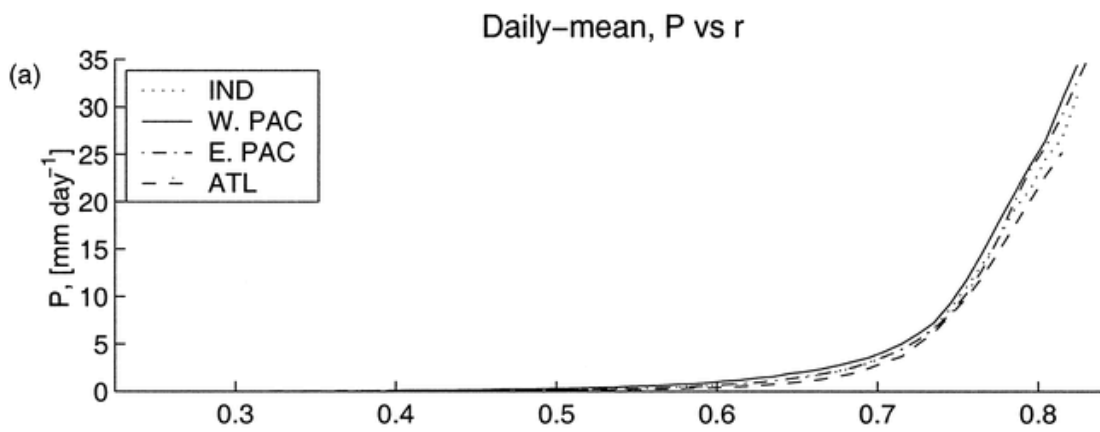


Figure C6 (Fig 3a in Bretherton et al., 2004): Mean daily averaged precipitation P in 1% bins of column relative humidity r for the four tropical ocean regions in their study.